J|A|C|S
ARTICLES
Published on Web 02/01/2006

# Di-organoiron Mixed Valent Complexes Featuring "($\eta^2$-dppe)($\eta^5$-$C_5Me_5$)Fe" Endgroups: Smooth Class-III to Class-II Transition Induced by Successive Insertion of 1,4-Phenylene Units in a Butadiyne-Diyl Bridge

Safaa Ibn Ghazala,[†] Frédéric Paul,*[,†] Loic Toupet,[‡] Thierry Roisnel,[§] Philippe Hapiot,[||] and Claude Lapinte*[,†]

*Contribution from Organométalliques et Catalyse: Chimie et Electrochimie Moléculaires, UMR CNRS 6509, Institut de Chimie, Université de Rennes I, Campus de Beaulieu, Bât. 10C, 35042 Rennes Cedex, France, Groupe Matière Condensée et Matériaux, UMR CNRS 6626, Université de Rennes I, Campus de Beaulieu, 35042 Rennes Cedex, France, Laboratoire de Chimie du Solide et Inorganique Moléculaire, UMR CNRS 6511, Institut de Chimie, Université de Rennes I, Campus de Beaulieu, 35042 Rennes Cedex, France, and Synthèse et Electrosynthèse Organique, UMR CNRS 6510, Institut de Chimie, Université de Rennes I, Campus de Beaulieu, 35042 Rennes Cedex, France*

Received November 10, 2005; E-mail: frederic.paul@univ-rennes1.fr; claude.lapinte@univ-rennes1.fr

***Abstract:*** The synthesis and study of a new redox family of symmetric dinuclear iron(II/III) complexes featuring "($\eta^2$-dppe)($\eta^5$-$C_5Me_5$)Fe(C≡C)" endgroups connected by a bis(diethynyl)-4,4′-biphenyl spacer are reported. The solid-state structures were determined (X-rays) for the homovalent Fe(II)/Fe(II) and Fe(III)/Fe(III) parents. In contrast, the mixed valent (MV) complex **5**[$PF_6$] has a low thermodynamic stability (Kc around 10) and cannot be isolated in a pure form, but was studied in solution. According to the Robin and Day classification, it constitutes a remarkable example of well-behaved weakly coupled class-II *organometallic* MV compound. The photodriven metal−metal electron-transfer process takes place over ca. 16 Å and corresponds to an electronic coupling of ca. 150 $cm^{-1}$ with a reorganization energy of ca. 6250 $cm^{-1}$ in dichloromethane. A similar investigation was also conducted in the near-IR range for the known and much more stable MV analogue **3**[$PF_6$] featuring the 1,4-phenyl unit instead of the 4,4′-biphenyl one ($K_c$ = 2.6 $10^4$). The latter also exhibits a localized valency, but presents a very intense intervalence charge-transfer band (IVCT) with a cutoff on the low-energy side. A much stronger electronic coupling is derived (ca. 1700 $cm^{-1}$) from the band shape for this MV complex in the frame of the two-level model. Although slowed, the electron exchange is not disrupted by insertion of an additional *para*-phenylene moiety into a 1,4-diethynylaryl bridge. Thus, starting from a compound with a butadiyne-diyl spacer, stepwise *para*-phenylene insertions in the bridge produce a smooth Class-III to Class-II transition for the corresponding MV complexes.

## Introduction

In the emerging field of molecular electronics,[1] polynuclear carbon-rich complexes featuring the electron-rich and redox-active organometallic endgroups appear particularly interesting from various perpectives, notably concerning information storage and processing.[2−6] From this point of view, the control (and understanding) of electron transfer over nanometric distances in a single molecule constitutes a decisive achievement. Accordingly, this area constitutes the center of active research from various groups involved in carbon-rich organometallics over the world.[4−7] In this respect, dinuclear organoiron MV complexes where two "($\eta^2$-dppe)($\eta^5$-$C_5Me_5$)Fe" redox-active termini are connected by a carbon-rich unsaturated spacer appear particularly appealing as molecular wire models to study the bridge properties.[8]

Since the seminal investigations on the Creutz−Taube salt,[9] the spectroscopic study of dinuclear mixed-valent compounds in the near-IR region has become a very useful way to get decisive information on the electron-transfer process in MV compounds and thereby also on the capability of a given bridge to convey electrons.[5,10−13] In most cases, the so-called Hush model (or two-level model) initially developed by Hush in 1967[14] furnishes simple spectral criteria to categorize a given MV complex according to the classification proposed the same year by Robin and Day,[15] and subsequently implemented by other researchers.[16]

As also established by others for related families of MV compounds,[12] we have shown that the polyyne bridge favors

[†] Organométalliques et Catalyse.
[‡] Groupe Matière Condensée et Matériaux.
[§] Laboratoire de Chimie du Solide et Inorganique Moléculaire.
[||] Synthèse et Electrosynthèse Organique.

(1) (a) Robertson, N.; Mc. Gowan, G. A. *Chem. Soc. Rev.* **2003**, *32*, 96−103. (b) Caroll, R. L.; Gorman, C. B. *Angew. Chem., Int. Ed. Engl.* **2002**, *41*, 4379−4400. (c) Tour, J. M. *Acc. Chem. Res.* **2000**, *33*, 791−803.

***Chart 1***

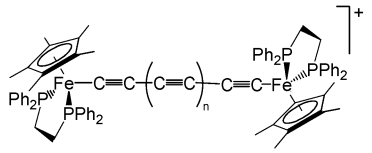

**1a**$^+$ (n = 0)
**1b**$^+$ (n = 1)
**1c**$^+$ (n = 2)

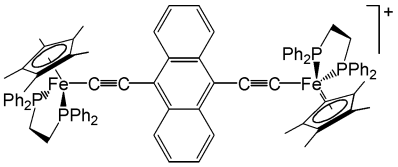

**2**$^+$

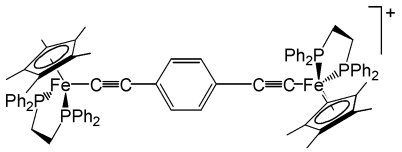

**3**$^+$

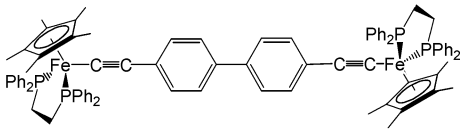

**5**

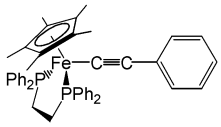

**4**

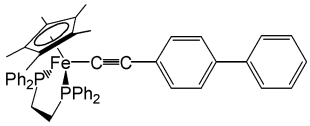

**6**

very efficient electronic delocalization between the two metallic centers in MV complexes **1a**−**c**$^+$ (Chart 1).[8a,17] Such MV complexes were previously categorized as Class-IIIA (**1a**$^+$) or borderline Class-II/Class-III. However, beyond eight carbon atoms, the MV complexes become more and more unstable from a kinetic standpoint and new structural variations have to be devised in order to stabilize MV with longer bridges. We have therefore started to investigate the use of aryl- and polyaryl units in a systematic fashion.[8a,18,19]

Arylene−ethynylene units are usually quite more stable kinetically than corresponding heteroaryl−ethynylene units[20,21] and often allow an easy synthetic access to the desired organoiron compounds, given the large number of aryl-based (catalytic) cross-coupling protocols available.[22,23] Moreover, depending on the connectivity of the aryl units, various nonlinear rigid geometries can be envisioned for the carbon-rich spacers incorporating such units. However, as each structural variation deeply modifies the electronic properties of the spacer and thereby strongly affects the communication between the redox-active endgroups, the effect of any such modification has to be studied carefully. Thus, the inclusion of a 1,4-phenylene unit into a polyyne-diyl bridge was shown to depress the electronic transfer in the MV state **3**[$PF_6$] in comparison to a pure polyyne-diyl bridge of same number of carbon atoms such as **1c**[$PF_6$],[8a,24]


(2) See for instance: (a) Cifuentes, M. P.; Humphrey, M. G.; Morall, J. P.; Samoc, M.; Paul, F.; Roisnel, T.; Lapinte, C. *Organometallics* **2005**, *24*, 4280−4288. (b) Hu, Q. Y.; Lu, W. X.; Tang, H. D.; Sung, H. H. Y.; Wen, T. B.; Williams, I. D.; Wong, G. K. L.; Lin, Z.; Jia, G. *Organometallics* **2005**, *24*, 3966−3973. (c) Fillaut, J.-L.; Perruchon, J.; Blanchard, P.; Roncali, J.; Gohlen, S.; Allain, M.; Migalska-Zalas, A.; Kityk, I. V.; Sahraoui, B. *Organometallics* **2005**, *24*, 687−695. (d) Venkatesan, K.; Blacque, O.; Fox, T.; Alfonso, M.; Schmalle, H. W.; Berke, H. *Organometallics* **2004**, *23*, 1183−1186. (e) Jiao, J.; Long, G. J.; Grandjean, F.; Beatty, A. M.; Fehlner, T. P. *J. Am. Chem. Soc.* **2003**, *125*, 7522−7523. (f) Wong, K. M.-C.; Lam, S. C.-F.; Ko, C.-C.; Zhu, N.; Yam, V. W.-W.; Roué, S.; Lapinte, C.; Fathallah, S.; Costuas, K.; Kahlal, S.; Halet, J.-F. *Inorg. Chem.* **2003**, *42*, 7086−7097. (g) Powell, C. E.; Humphrey, M. G.; Cifuentes, M. P.; Morall, J. P.; Samoc, M.; Luther-Davies, B. *J. Phys. Chem. A* **2003**, *107*, 11264−11266. (h) Naklicki, M. L.; White, C. A.; Plante, L. L.; Evans, C. E. B.; Crutchley, R. J. *Inorg. Chem.* **1998**, *37*, 1880−1885.

(3) Recent general references on properties of carbon-rich organometallics: (a) Rigaut, S.; Touchard, D.; Dixneuf, P. H. *Coord. Chem. Rev.* **2004**, *248*, 1585−1601. (b) Bruce, M. I.; Low, P. J. *Adv. Organomet. Chem.* **2004**, *50*, 179−444S. (c) Szafert, S.; Gladysz, J. A. *Chem. Rev.* **2003**, *103*, 4175−4205. (d) Yam, V. W.-W. *Acc. Chem. Res.* **2002**, *35*, 555−563. (e) Powell, C. E.; Humphrey, M. G. *Coord. Chem. Rev.* **2004**, *248*, 725−756.

(4) Ren, T. *Organometallics* **2005**, *24*, 4854−4870.

(5) Crutchley, R. J. *Adv. Inorg. Chem.* **1994**, *41*, 273−325.

(6) (a) Schwab, P. F. H.; Levin, M. D.; Michl, J. *Chem. Rev.* **1999**, *99*, 1863−1933. (b) Schwab, P. F. H.; Smith, J. R.; Michl, J. *Chem. Rev.* **2005**, *105*, 1197−1279.

(7) See for instance; (a) Qi, H.; Gupta, A.; Noll, B. C.; Snider, G. L.; Lu, Y.; Lent, S. S.; Fehlner, T. P. *J. Am. Chem. Soc.* **2005**, *127*, 15218−15227. (b) Blum, A. S.; Ren, T.; Parish, D. A.; Trammell, S. A.; Moore, M. H.; J. G. Kushmerick; Xu, G.-L.; Deschamps, J. R.; Polack, S. K.; Shashidar, R. *J. Am. Chem. Soc.* **2005**, *127*, 10010−10011. (c) Xu, G.-L.; Crutchley, R. J.; DeRosa, M. C.; Pan, Q.-J.; Zhang, H.-X.; Wang, X.; Ren, T. *J. Am. Chem. Soc.* **2005**, *127*, 13354−13365. (d) Schull, T. L.; Kushmerick, J. G.; Patterson, C. H.; George, C.; Moore, M. H.; Pollack, S. K.; Shashidhar, R. *J. Am. Chem. Soc.* **2003**, *125*, 3202−3203.

(8) (a) Paul, F.; Lapinte, C. *Coord. Chem. Rev.* **1998**, *178/180*, 427−505. (b) Paul, F.; Lapinte, C. In *Unusual Structures and Physical Properties in Organometallic Chemistry*; Gielen, M., Willem, R., Wrackmeyer, B., Eds.; Wiley & Sons: Ldt: San-Francisco, 2002, pp 219−295.

(9) Creutz, C.; Taube, H. *J. Am. Chem. Soc.* **1973**, *95*, 1086−1094.

(10) Demadis, K. D.; Hartshorn, C. M.; Meyer, T. J. *Chem. Rev.* **2001**, *101*, 2655−2685.

(11) Nelsen, S. F. *Chem. Eur. J.* **2000**, *4*, 581−588.

(12) (a) Launay, J.-P. *Chem. Soc. Rev.* **2001**, *30*, 386-397. (b) Launay, J.-P.; Coudret, C. In *Electron Transfer in Chemistry*; Balzani, V., de Silva, A. P., Eds.; Wiley-VCH: 2000; Vol. 5, pp 3−47.

(13) (a) Ward, M. D. *Chem. Ind.* **1996**, 568−573. (b) Ward, M. D. *Chem. Soc. Rev.* **1995**, *24*, 121−134.

(14) (a) Hush, N. S. *Prog. Inorg. Chem.* **1967**, *8*, 357−389. (b) Hush, N. S. *Prog. Inorg. Chem.* **1967**, *8*, 391−444.

(15) Robin, M. B.; Day, P. *Adv. Inorg. Chem. Radiochem.* **1967**, 247−422.

(16) (a) Brunschwig, B. S.; Creutz, C.; Sutin, N. *Chem. Soc. Rev.* **2002**, *31*, 168−184. (b) Creutz, C.; Newton, M. D.; Sutin, N. *J. Photochem. Photobiol. A.* **1994**, *82*, 47−59.

(17) (a) Coat, F.; Paul, F.; Lapinte, C.; Toupet, L.; Costuas, K.; Halet, J.-F. *J. Organomet. Chem.* **2003**, *683*, 368−378. (b) Le Narvor, N.; Toupet, L.; Lapinte, C. *J. Am. Chem. Soc.* **1995**, *117*, 7129−7138.

(18) (a) Weyland, T.; Costuas, K.; Toupet, L.; Halet, J.-F.; Lapinte, C. *Organometallics* **2000**, *19*, 4228−4239. (b) Weyland, T.; Costuas, K.; Mari, A.; Halet, J.-F.; Lapinte, C. *Organometallics* **1998**, *17*, 5569−5579. (c) Weyland, T.; Lapinte, C.; Frapper, G.; Calhorda, M. J.; Halet, J.-F.; Toupet, L. *Organometallics* **1997**, *16*, 2024−2031.

(19) de Montigny, F.; Argouarch, G.; Costuas, K.; Halet, J.-F.; Roisnel, T.; Toupet, L.; Lapinte, C. *Organometallics* **2005**, *24*, 4558−4572.

(20) (a) Roué, S.; Lapinte, C. *J. Organomet. Chem.* **2005**, *690*, 594−604. (b) Le Stang, S.; Paul, F.; Lapinte, C. *Organometallics* **2000**, *19*, 1035−1043.

(21) Lapinte, C., unpublished results.

(22) Diederich, F.; Stang, P. J. *Metal-Catalyzed Cross-Coupling Reactions*; Wiley-VCH Verlag GmbH: Weinheim, 1998.

(23) (a) Courmarcel, J.; Le Gland, G.; Toupet, L.; Paul, F.; Lapinte, C. *J. Organomet. Chem.* **2003**, *670*, 108−122. (b) Denis, R.; Weyland, T.; Paul, F.; Lapinte, C. *J. Organomet. Chem.* **1997**, *545/546*, 615−618.

***Scheme 1***

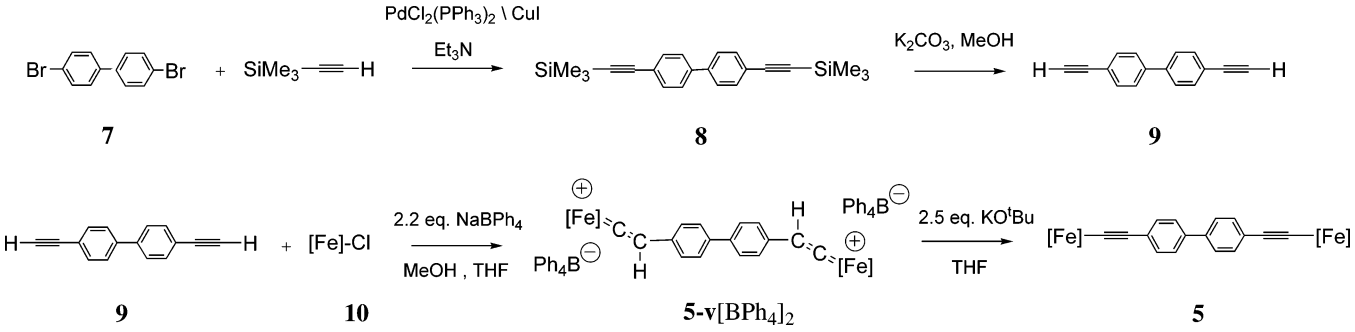


***Table 1.*** Infrared Data for Selected Complexes in $CH_2Cl_2$ Solution ($cm^{-1}$)[a]

| cpnd | Fe(II) $\nu_{C\equiv C}$ | Fe(II)/Fe(III) $\nu_{C\equiv C}$ | Fe(III) $\nu_{C\equiv C}$ | $\Delta\nu_{C\equiv C}$[b] Fe(II)/Fe(III) | ref |
|---|---|---|---|---|---|
| [Fe]C≡C−$(C_6H_4)_2$−C≡C[Fe] (**5**) | 2051 | 2043<br>1979 | 1991 | −60 | this work |
| [Fe]C≡C−$C_6H_4$−$C_6H_5$ (**6**) | 2052 | / | 1991 | −61 | this work |
| [Fe]C≡C−$C_6H_4$−C≡C[Fe] (**3**) | 2051 | 2016<br>1934 | 1987 | −64 | this work |
| [Fe]C≡CPh (**4**) | 2053 | / | 2021<br>1988 | −49[c] | 29 |

[Fe] ≡ ($\eta^2$-dppe)($\eta^5$-$C_5Me_5$)Fe. [a] Solid state $\nu_{C\equiv C}$ values obtained in KBr for isolated complexes are given in the Experimental Section. [b] Fe(II) vs Fe(III) $\nu_{C\equiv C}$ difference ($PF_6^-$ counterion). [c] Mean difference: two bands were observed for the Fe(III) parent, presumably due to Fermi coupling.[29]

while the 9,10-anthryl unit in **2**[$PF_6$] recently appeared as a promising alternative to this unit regarding electronic delocalization.[19]

Further cis-insertion of 1,4-phenylene units in the bridge was next envisioned as a straightforward way to obtain MV complexes with extended bridges. However, a dramatic decrease in the electronic coupling was expected for these compounds,[12a,25] especially with "($\eta^2$-dppe)($\eta^5$-$C_5Me_5$)Fe" endgroups prone to exhibit highly metal-centered frontier molecular orbitals.[26,27] This was also more likely considering the existence of various conformers with nonplanar bridge conformations, evidently less favorable to the electron-transfer process.[12a,28] The study of the complex **5**[$PF_6$] featuring a 2,2′-biphenyl unit in the bridge (Chart 1) revealed a quite larger electronic coupling than anticipated. More remarkably, we presently show that a progressive transition from class-III to class-II can be achieved by successive 1,4-phenylene insertions in the carbon-rich bridge, when proceeding from **1a**[$PF_6$] to **5**[$PF_6$]. For the first time, we also provide here an interpretation of the complex band shape of the intervalence charge transfer band (IVCT) in strongly coupled compounds such as **3**[$PF_6$]. Accordingly, the reader will find in the following (i) the synthesis and characterization of the new redox family of dinuclear complexes **5**/**5**$^+$/**5**$^{2+}$ and of the corresponding new family of mononuclear complexes **6**/**6**$^+$, used as benchmarks for the characterization of **5**/**5**$^+$/**5**$^{2+}$, (ii) the study of the MV complex **5**[$PF_6$] in the near-IR domain along with that of the known MV complex **3**[$PF_6$] in the same spectral range for comparison purposes and (iii) a short discussion on the evolution of the electronic coupling ($H_{ab}$) between these and related MV complexes such as **1a**[$PF_6$] or **2**[$PF_6$].

## Results and Discussion

**Synthesis and Characterization of the New Organoiron(II) Complexes.** The synthesis of the desired dinuclear Fe(II) complex **5** was achieved following the reaction sequence depicted in Scheme 1. The trimethylsilyl-protected organic precursor **8** of the bridge was classically obtained following a Sonogashira coupling procedure from the commercial 4,4′-dibromo-1,1′-biphenyl **7** (95%). This compound was then deprotected with potassium carbonate giving the terminal bis-alkyne **9** in good yields (93%). The latter was reacted with the chloride complex ($\eta^2$-dppe)($\eta^5$-$C_5H_5$)FeCl (**10**) to form the corresponding bis-vinylidene complex **5-v**[$BPh_4$]$_2$, which was only briefly characterized by NMR and infrared spectroscopies before being deprotonated in situ to give **5** in 63% overall yield.

This complex has a poor solubility in most organic solvents, but could nevertheless be fully characterized by NMR, by ESI−MS, and a satisfactory elemental analysis was obtained. $^{31}P$ NMR reveal the highly symmetric nature of this compound, and the single signal observed at 101.1 ppm is characteristic of an acetylide Fe(II) complex. The proton spectrum clearly confirms the expected 1−1 ratio between the $C_5Me_5$ ligand and 1,4-phenylene units. Due to the very low solubility of the complex mentioned above, the characteristic triplet ($^2J_{CP}$ ca. 40 Hz) and singlet signatures for the symmetric acetylide linkage could only be detected with difficulty at 142.3 and 120.4 ppm by $^{13}C$ NMR, respectively.[18c,26] As for the 1,4-phenyl analogue **3**, a single stretching frequency is detected for the two alkynyl units at very similar wavenumbers (Table 1), which are also very close to the value recorded for the corresponding mononuclear complex **4**. Notably, Raman spectroscopy reveals that the weak absorption observed at 1949 $cm^{-1}$ (Figure 1) does not correspond to the symmetric $\nu_{C\equiv C}$ mode.[29] This infrared absorption rather corresponds to a combination or harmonic

(24) Le Narvor, N.; Lapinte, C. *Organometallics* **1995**, *14*, 634−639.
(25) Kim, Y.; Lieber, C. M. *Inorg. Chem.* **1989**, *28*, 3990−3992.
(26) (a) Costuas, K.; Paul, F.; Toupet, L.; Halet, J.-F.; Lapinte, C. *Organometallics* **2004**, *23*, 2053−2068. (b) Denis, R.; Toupet, L.; Paul, F.; Lapinte, C. *Organometallics* **2000**, *19*, 4240−4251.
(27) Paul, F.; Toupet, L.; Thépot, J.-Y.; Costuas, K.; Halet, J.-F.; Lapinte, C. *Organometallics* **2005**, *24*, 5464−5478.
(28) Woitellier, S.; Launay, J.-P.; Joachim, C. *Chem. Phys.* **1989**, *131*, 481−488.

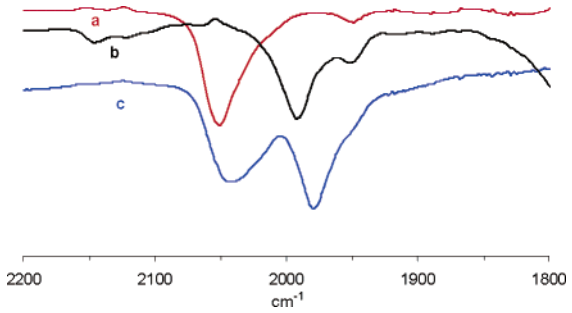


***Figure 1.*** Infrared spectra for **5** (a) and $\mathbf{5}^{2+}$ (b) complexes and for an equimolar mixture of **5** and $\mathbf{5}^{2+}$ (c) in dichloromethane (KBr window).

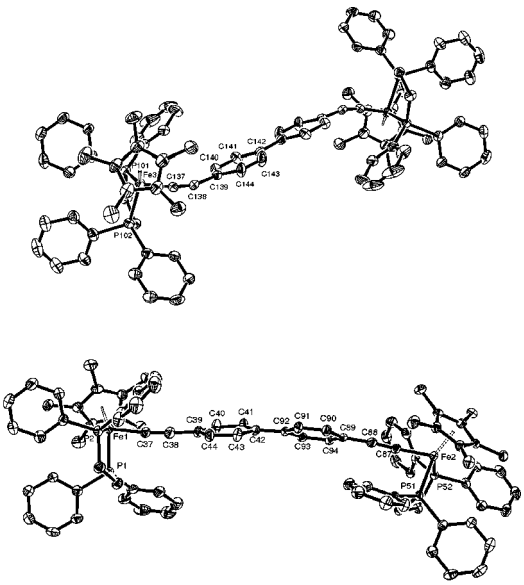

***Figure 2.*** ORTEP representations of the two conformations of complex **5** in the asymmetric units at 50% probability level.

mode. Comparison with the infrared data obtained for **3** (Table 1) suggest that the introduction of a second 1,4-phenylene unit does not markedly perturb the $\nu_{C\equiv C}$ stretches. Thus, the vibronic coupling between the $\nu_{C\equiv C}$ through the phenylene linker must remain relatively small in both complexes.

Finally, very small red crystals could be grown from THF-pentane mixtures for **5** and a X-ray structure could be obtained which confirms the identity of the compound (see Figure 2).

The synthesis of the mononuclear Fe(II) acetylide complex **6** containing the 4-biphenyl unit was realized following a similar reaction sequence (Scheme 2). Again, a Sonogashira procedure was used to generate the silyl-protected biphenyl acetylene **12** from commercial 4-bromobiphenyl (**11**), followed by a desilylation step. The resulting alkyne (**13**) was reacted with the

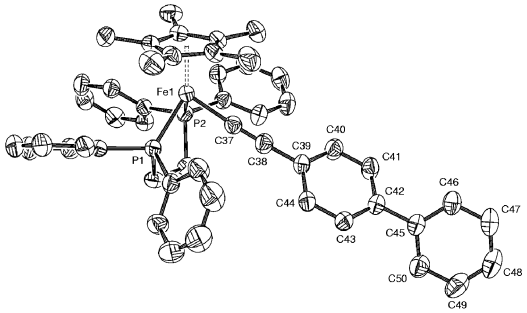

***Figure 3.*** ORTEP representations of complex **6** at 50% probability level.

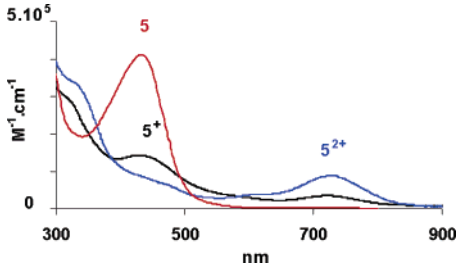


***Figure 4.*** UV-vis spectra for **5** and $\mathbf{5}^{2+}$ complexes and for an equimolar mixture of **5** and $\mathbf{5}^{2+}$ in dichloromethane.

chloride complex **10** to give the vinylidene complex **6-v**[$PF_6$] which was subsequently deprotonated in situ. This complex was fully characterized by usual spectroscopies, by ESI−MS, and a satisfactory elemental analysis was obtained as well. $^{31}$P NMR gives the characteristic singlet at 101.5 ppm expected for an acetylide Fe(II) complex, while the acetylide linkage is signaled by a characteristic triplet ($^2J_{CP}$ = 39 Hz) and singlet at 139.3 and 121.0 ppm, respectively, in the $^{13}$C NMR spectrum. A single stretching frequency is also detected at 2056 cm$^{-1}$ for the $\nu_{C\equiv C}$ (Table 1). In addition, red crystals could be grown from dichloromethane/*n*-pentane mixtures and the structure of **6** could be solved (Figure 3).

The UV−vis spectra of these new compounds were recorded (Table 2). For each of them, a broad absorption was observed near 410 nm, which corresponds to a MLCT band (Figure 4).[26] Accordingly, this band is not found on the absorption spectrum of the silylated organic bridge precursor. The MLCT absorption for **5** is bathochromically shifted by 30 nm relative to **6**, as expected from the more electron-rich nature of the dinuclear complex, resulting in more energetic filled (donor) d metal-centered nonbonding MOs and thereby in closer MLCT (excited) states.

**Cyclic Voltammetry.** Cyclic voltammograms were recorded for the oxidation of the dinuclear compounds **5** and **6**, and

***Scheme 2***

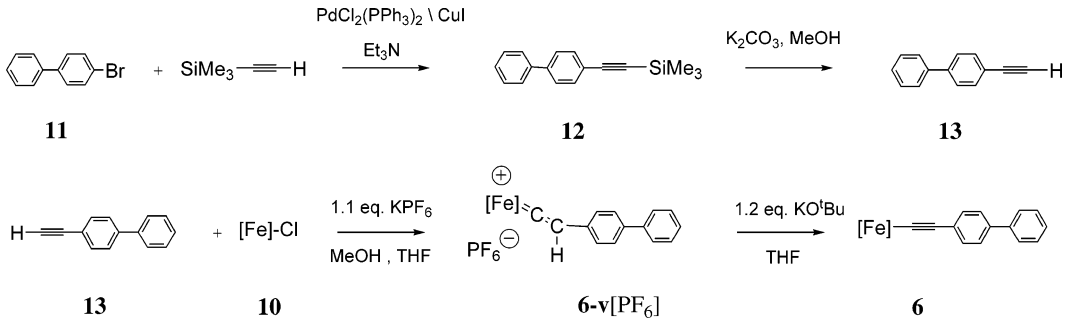

***Table 2.*** UV-vis Data for Selected Fe(II) and Fe(III) Complexes in $CH_2Cl_2$

| cpnd | absorptions in nm ($10^{-3}\epsilon$ in $M^{-1}$ $cm^{-1}$) | ref |
|---|---|---|
| $Me_3Si-C\equiv C-(C_6H_4)_2-C\equiv C-SiMe_3$ (**7**) | 303 (37.5) | this work |
| $[Fe]C\equiv C-(C_6H_4)_2-C\equiv C[Fe]$ (**5**) | 275 (sh, 42.9), 432 (40.2) | this work |
| $\{[Fe]C\equiv C-(C_6H_4)_2-C\equiv C[Fe]\}^{2+}$ (**5**$^{2+}$) | 278 (sh, 50.4), 334 (sh, 33.0), 464 (sh, 6.8), 623 (3.8), 726 (8.4) | this work |
| $[Fe]C\equiv C-C_6H_4-C_6H_5$ (**6**) | 275 (sh, 34.1), 401 (17.5) | this work |
| $[[Fe]C\equiv C-C_6H_4-C_6H_5]^+$ (**6**$^+$) | 280 (sh, 88.2), 370 (sh, 7.2), 440 (sh, 3.0), 613 (2.0), 710 (4.1) | this work |
| $[Fe]C\equiv C-C_6H_4-C\equiv C[Fe]$ (**3**) | 261 (sh, 34.7), 395 (sh, 24.2), 411 (25.4), 525 (3.4) | this work |
| $\{[Fe]C\equiv C-C_6H_4-C\equiv C[Fe]\}^+$ (**3**$^+$) | 264 (sh, 46.8), 424 (8.7), 547 (17.0), 702 (7.6) | this work |
| $\{[Fe]C\equiv C-C_6H_4-C\equiv C[Fe]\}^{2+}$ (**3**$^{2+}$) | 275 (sh, 51.1), 420 (8.0), 619 (sh, 5.4), 702 (42.8), 769 (sh, 7.1) | this work |
| $[Fe]C\equiv CPh$ (**4**) | 277 (sh, 14.5), 350 (13.6) | 26b |
| $\{[Fe]C\equiv CPh\}^+$ (**4**$^+$) | 261 (sh, 32.6); 280 (sh, 27.4); 301 (sh, 18.8); 342 (sh, 5.9); 379 (sh, 3.6); 575 (sh, 2.3); 662 (3.1) | 27 |

[Fe] ≡ ($\eta^2$-dppe)($\eta^5$-$C_5Me_5$)Fe.

***Table 3.*** Electrochemical Data for Selected Complexes

| cpnd | $E°$ (V)[a] | $\Delta E°$ (V) | $i_c/i_a$ | ref |
|---|---|---|---|---|
| $[Fe]C\equiv C-(C_6H_4)_2-C\equiv C[Fe]$ (**5**) | −0.17[b] | 0.06 | 1 | this work |
| | −0.11[b] | | 1 | |
| $[Fe]C\equiv C-C_6H_4-C_6H_5$ (**6**) | −0.16 | / | 1 | this work |
| $[Fe]C\equiv C-C_6H_4-C\equiv C[Fe]$ (**3**) | −0.27 [c] | 0.26 | 1 | 8a |
| | −0.01 [c] | | 1 | |
| $[Fe]C\equiv CPh$ (**4**) | −0.15 | / | 1 | 26 |

[Fe] ≡ ($\eta^2$-dppe)($\eta^5$-$C_5Me_5$)Fe. [a] All $E$ values in V vs SCE Conditions: $CH_2Cl_2$ solvent, 0.1 M ($N^nBu_4$)($PF_6$) supporting electrolyte, 20 °C, Pt electrode, sweep rate 0.100 V $s^{-1}$. The ferrocene/ferricinium ($Fc/Fc^+$) complex was used as an internal reference for potential measurements. [b] E° values extracted by simulation. [c] E° values presently corrected for $Fc/Fc^+$ at 0.460 V vs SCE in $CH_2Cl_2$.[33]

compared to the results obtained for mononuclear complexes **3** and **4** (Table 3). Two separate monoelectronic and reversible waves are observed for **3** in contrast to **5**, which exhibits a single two-electron reversible wave. The determination of the two standard potentials $E°_1$ and $E°_2$ is straightforward in the case of two separated waves. These can be derived as the midpoints between the anodic and cathodic peaks of each one-electron wave. In the case of a single two-electron wave, as observed for **5**, the two standard potentials can also be derived from the location of the midpoint between the anodic and cathodic peaks and the distance between them ($\Delta E_p$), provided the kinetics of the electron-transfer processes do not affect the cyclic voltammetric response.[30−32] This condition was checked by investigating the variation of $\Delta E_p$ as a function of the scan rate, and we found that only negligible variations are observed for scan rates below 1 V·$s^{-1}$. Thus, $\Delta E_p$ tends toward a limit (85 mV) that corresponds to the thermodynamics of the electron-transfer processes which leads to a difference $\Delta E°$ (V) = 62 mV (use of a working curve after simulation of the voltammogram), evidencing that the equilibrium constant for the comproportionation reaction (equation 1) is around 11−12 for **5** (see Supporting Information). This is quite close to the statistical value of 4 and reflects the weak intramolecular electronic interaction taking place between the two metal end-groups in the MV compound **5**$^+$. For complex **6**, one redox wave corresponding to the Fe(III/II) oxidation is observed at −0.16 V vs ECS. Expectedly, this potential is very close to the first oxidation potential $E°_1$ of **5** (ca. −0.17 V), in line with a more difficult oxidation process for the mononuclear complex, which is slightly less electron-rich than the dinuclear relative.

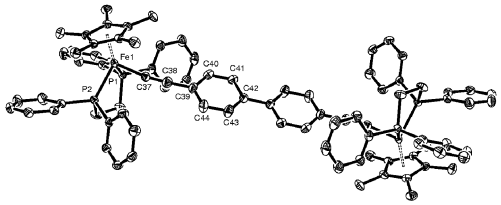


***Figure 5.*** ORTEP representations of complex **5**$^{2+}$ at 50% probability level.

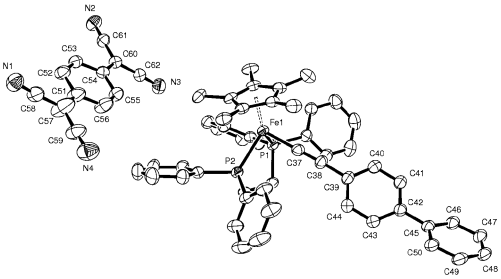


***Figure 6.*** ORTEP representations of complex **6**[TCNQ] at 50% probability level.

$$5 + 5^{++} \rightleftarrows 5^+ + 5^+ \qquad (1)$$

It is also interesting to note that the small variation of $\Delta E_p$ with the scan rate (<1 V.$s^{-1}$) indicates that the kinetics of the electron transfer are relatively fast,[31] and thus, that the reorganization energies associated with the change of the redox state are small, as expected from previous work on related compounds.[26a]

**Synthesis and Characterization of Organoiron(III) Complexes.** The isolation of the corresponding mono- and dioxidized Fe(III) congeners **6**$^+$ and **5**$^{2+}$ was achieved from **6** and **5** by chemical oxidation using 1 and 2 equiv. of ferricinium hexafluorophosphate, respectively (Scheme 3).

Small dark crystals could be grown from dichloromethane/*n*-pentane mixtures for **5**$[PF_6]_2$ and a X-ray structure could be obtained which confirms the identity of the compound (see Figure 5). Using TCNQ as an oxidant in place of ferricinium hexafluorophosphate allowed the isolation of **6**[TCNQ]. Dark green crystals of this compound could be grown from dichloromethane/*n*-pentane mixtures, and the solid-state structure was solved (Figure 6).

These green Fe(III) complexes were characterized by infrared spectroscopy (Table 1) and cyclic voltammetry. For all Fe(III) complexes, a single weak $\nu_{C\equiv C}$ is observed near 1990 $cm^{-1}$, in

(29) Paul, F.; Mevellec, J.-Y.; Lapinte, C. *J. Chem. Soc., Dalton Trans.* **2002**, 1783−1790.
(30) Myers, R. L.; Shain, I. *Anal. Chem.* **1969**, *41*, 980.
(31) (a) Hapiot, P.; Kispert, L. D.; Konovalov, V. V.; Saveant, J.-M. *J. Am. Chem. Soc.* **2001**, *123*, 6669−6677. (b) Andrieux, C. P.; Savéant, J.-M. *J. Electroanal. Chem.* **1974**, *57*, 27−33.
(32) Guerro, M.; Carlier, R.; Boubekeur, K.; Lorcy, D.; Hapiot, P. *J. Am. Chem. Soc.* **2003**, *125*, 3159−3167.

*Scheme 3*

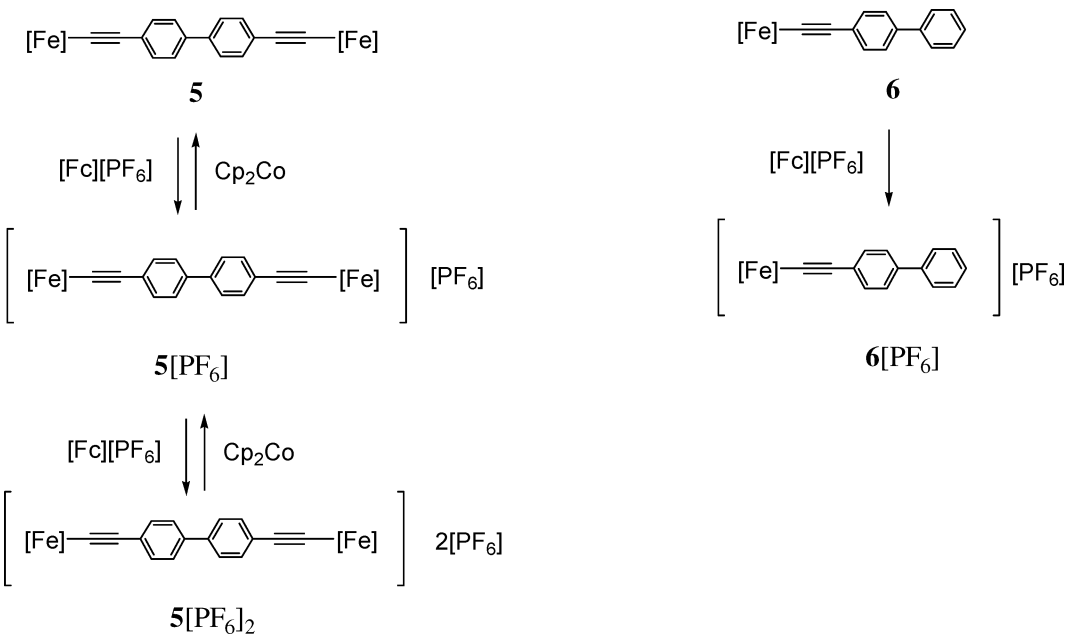


***Table 4.*** ESR spectra for compounds in frozen $CH_2Cl_2$/1,2-$C_2H_4Cl_2$ solutions at 80 K

| cpnd | $g_1$ | $g_2$ | $g_3$ | $\Delta g$ | ref |
|---|---|---|---|---|---|
| $\{[Fe]C\equiv C\text{-}(C_6H_4)_2\text{-}C\equiv C[Fe]\}^{2+}$ ($\mathbf{5}^{2+}$) | 2.035 ($\Delta H_{pp}$ ca. 160 G)[a] | | | / | this work |
| $\{[Fe]C\equiv C\text{-}(C_6H_4)_2\text{-}C\equiv C[Fe]\}^{+}$ ($\mathbf{5}^{+}$) | 2.418 | 2.134 | 1.976 | 0.442 | this work |
| $[[Fe]C\equiv C\text{-}C_6H_4\text{-}C_6H_5]^{+}$ ($\mathbf{6}^{+}$) | 2.439 | 2.032 | 1.975 | 0.464 | this work |
| $\{[Fe]C\equiv C\text{-}C_6H_4\text{-}C\equiv C[Fe]\}^{2+}$ ($\mathbf{3}^{2+}$) | 2.032 ($\Delta H_{pp}$ ca. 160 G)[a] | | | / | this work |
| $\{[Fe]C\equiv C\text{-}C_6H_4\text{-}C\equiv C[Fe]\}^{+}$ ($\mathbf{3}^{+}$) | 2.199 | 2.049 | 2.031 | 0.168 | 24 |
| $\{[Fe]C\equiv CPh\}^{+}$ ($\mathbf{4}^{+}$) | 2.464 | 2.033 | 1.975 | 0.489 | 27,34 |

[Fe] ≡ ($\eta^2$-dppe)($\eta^5$-$C_5Me_5$)Fe. [a] Pure solid sample of $\mathbf{5}^{2+}$ (no signal corresponding to a hypothetical forbidden $\Delta m_s = 2$ transition detected around g = 4.5).

accordance with the expected decrease in acetylide bond order upon oxidation.[24,29] Again, Raman spectroscopy reveals that the weak absorption observed at 1952 $cm^{-1}$ (Figure 1) does not correspond to the symmetric stretching motion of the alkyne vibrators in $\mathbf{5}[PF_6]_2$.

The UV−vis spectra of these new compounds **5** and **6** were also recorded (Table 2). The broad absorption observed near 700 nm (Figure 4) which corresponds to a LMCT band in these Fe(III) compounds explains the darker color of the complexes.[27] This LMCT absorption is bathochromically shifted of ca. 20 nm for $\mathbf{5}^{2+}$ relative to $\mathbf{6}^{+}$, likewise to what was observed between **5** and **6**. This time, this trend can be rationalized by the dicationic nature of the $\mathbf{5}[PF_6]_2$, resulting in less energetic virtual (accepting) d MOs localized on the metal center, therefore in closer excited LMCT states.

The presence of unpaired electron(s) in $\mathbf{6}^{+}$ and in $\mathbf{5}^{2+}$ is confirmed by clear ESR signatures (Table 4 and Figure 7). Thus, a rhombic signal, typical of a metal-centered radical, was observed at 80° K in dichloromethane/1,2-dichloroethane glasses for $\mathbf{6}^{+}$, while a broad, seemingly isotropic, signal was obtained at the same temperature for $\mathbf{5}^{2+}$ at $g = 2.035$ ($\Delta H = 160$ G). Upon coming back to room temperature, this signal is still observed, but becomes thinner ($\Delta H = 60$ G) and shifts toward $g_e$. While the latter signal is not typical of metal centered radicals but is rather suggestive of an organic side-product, the spectra initially recorded at 77 K or obtained with pure solid samples of $\mathbf{5}^{2+}$ (Table 4, Figure 7) is clearly in line with ESR signatures previously obtained for related Fe(III)/Fe(III) diradicals.[18b]

The Mössbauer spectra also clearly reveal the change in the oxidation state of the iron centers between **5** and $\mathbf{5}[PF_6]_2$ as well as between **6** and $\mathbf{6}[PF_6]$ (Table 5). Indeed, while the slight differences in isomeric shift are less informative with such arylacetylide organoiron compounds,[26b] the quadrupolar splitting is nevertheless diagnostic of an Fe(II) center in **5** and **6**, and of an Fe(III) center in $\mathbf{5}[PF_6]_2$ and $\mathbf{6}[PF_6]$.[34,35] The $^1H$ NMR spectra of $\mathbf{5}[PF_6]_2$ and $\mathbf{6}[PF_6]$ are also very typical of paramagnetic Fe(III) complexes.[36,37] Notably, the characteristic broad cyclopentadiene resonance is located at ca. −10 ppm for both the $^1H$ NMR spectra of $\mathbf{5}[PF_6]_2$ and $\mathbf{6}[PF_6]$ in chloroform, which suggests the presence of roughly one unpaired electron on the metallic endgroups.[36] Indeed, for dinuclear Fe(III) complexes exhibiting strong antiferromagnetic coupling this resonance is usually detected at higher fields.[17b] Thus, while antiferromagnetic coupling between the unpaired spins is expected in $\mathbf{5}[PF_6]_2$ according to Ovchinnikov's rule[38] or molecular orbital (MO) considerations,[8b] the latter must be quite weak. In line with this hypothesis, Evans measurements in dichloromethane solution for $\mathbf{6}[PF_6]$ and $\mathbf{5}[PF_6]_2$ give 1.8 ± 0.4 $\mu_B$ and 2.7 ± 0.4 $\mu_B$, close to the values expected for doublet (1.73 $\mu_B$) and triplet

(33) Connelly, N. G.; Geiger, W. E. *Chem. Rev.* **1996**, *96*, 877−910.
(34) Connelly, N. G.; Gamasa, M. P.; Gimeno, J.; Lapinte, C.; Lastra, E.; Maher, J. P.; Le Narvor, N.; Rieger, A. L.; Rieger, P. H. *J. Chem. Soc., Dalton Trans.* **1993**, 2575−2578.
(35) Guillaume, V.; Thominot, P.; Coat, F.; Mari, A.; Lapinte, C. *J. Organomet. Chem.* **1998**, *565*, 75−80.
(36) Roger, C.; Hamon, P.; Toupet, L.; Rabaâ, H.; Saillard, J.-Y.; Hamon, J.-R.; Lapinte, C. *Organometallics* **1991**, *10*, 1045−1054.
(37) Paul, F., work in progress.

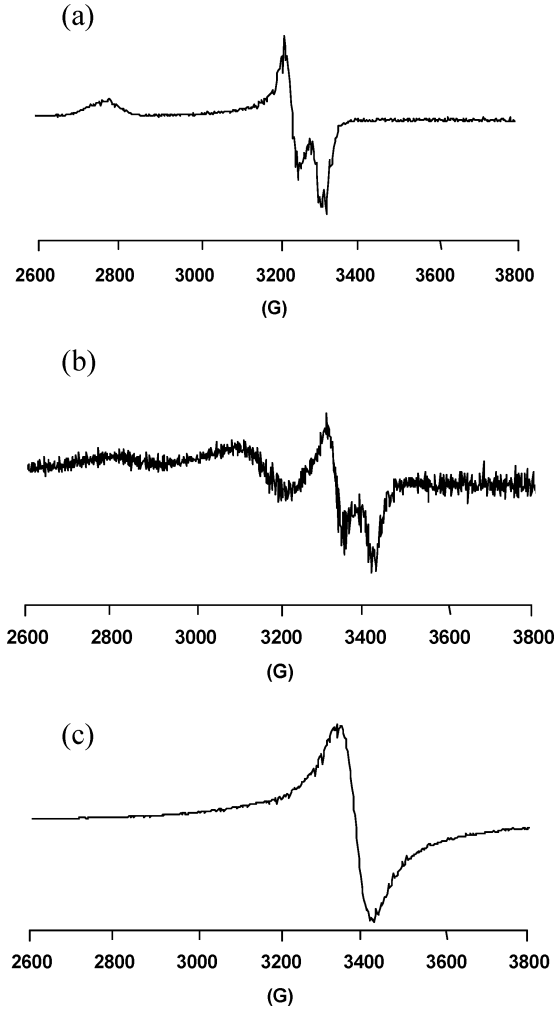


***Figure 7.*** ESR spectrum of (a) **6**[$PF_6$] and (b) a mixture of **5**[$PF_6$] and **5**[$PF_6$]$_2$ in 1,2-$CH_2Cl_2$/$C_2H_4Cl_2$ (1:1) at 80 K. (c) ESR spectrum of a pure solid sample of **5**[$PF_6$]$_2$ at 77 K.

(2.83 $\mu_B$) compounds, respectively, using the spin only formula (eq 2) and taking the free electron $g_e$ (= 2.023) value for $g$.[39] Thus, **5**[$PF_6$]$_2$ essentially behaves as an unpaired diradical in solution at ambient temperature in line with no or weak antiferromagnetic coupling between unpaired spins through the bis-4,4′-ethynyl-(1,1′-biphenyl) spacer. Note that in the case of **3**[$PF_6$]$_2$, the existence of antiferromagnetic coupling under similar conditions was previously suggested by Evans measurements and more firmly established by magnetic susceptibility measurements.[24,40]

$$\mu = g[S(S+1)]^{1/2} \qquad (2)$$

In the near-IR range, a weak and broad absorption is detected around 1850 nm (5400 $cm^{-1}$) for both compounds (Table 6). Both transitions take place roughly at the same energy than as previously observed for **4**[$PF_6$]. Thus, this absorption, absent in the Fe(II) precursors, likely corresponds to a forbidden ligand field (LF) transition localized at the Fe(III) end of the complexes (SOMO-2/SOMO transition).[18c,27,41] The transition in **5**[$PF_6$]$_2$ is therefore doubly degenerate. In line with this interpretation, the near-IR transition of complex **5**[$PF_6$]$_2$ exhibits roughly a doubled intensity in comparison to that of the mononuclear complex **6**[$PF_6$].

**X-ray Structures of 5, 5[$PF_6$]$_2$, 6 and 6[TCNQ].** The compound **5** (Figures 2) crystallizes in the P-1 symmetry group, with two molecules in the asymmetric unit (Table 7). The presence of two molecules with slightly different conformations and bond lengths in the asymmetric unit reveals the sizable structural influence of the packing on the molecular geometry. This suggests that some caution should be exercised when trying to interpret weak structural changes in terms of intramolecular influences only. Notably, this phenomenon *is not* connected to the presence of THF or *n*-pentane molecules as solvates, since a very similar solid state arrangement is observed in crystals grown from nitrobenzene-diethyl ether mixtures, but featuring only water molecules as solvates (see Supporting Information). The structure shows that the two aryl rings of the biphenyl are coplanar, despite the steric interactions existing between the 3,5- and 3′,5′- hydrogen atoms of the 4,4′-biphenyl spacer. Noteworthy, this phenomenon is observed for the two molecules in the asymmetric units *in the absence* of any $\pi$-stacking interactions between adjacent biphenyl moieties, well-known to stabilize such conformations in the solid state.[42] The corresponding dication **5**[$PF_6$]$_2$ (Figure 5) also crystallizes in the P-1 symmetry group, with one molecule in the asymmetric unit (Table 7). This solid-state structure again exhibits a coplanar conformation for the biphenyl spacer. The significant changes in bond lengths induced by oxidation include a slight expansion of the coordination spheres around the iron centers, as well a slight shortening of the Fe−C bond length (See Supporting Information). These changes closely match those stated for **6** and **6**[TCNQ] (see after). Also, note that for both **5** and **5**[$PF_6$]$_2$ the intramolecular Fe−Fe distances (16.18 and 16.11 Å, respectively) are longer than the shortest intermolecular Fe−Fe separations (8.75 and 10.64 Å respectively).

The mononuclear compounds **6** and **6**[TCNQ] (Figures 3 and 6) crystallize in the P-1 symmetry group, with two and one molecule(s) in the asymmetric unit (Table 7), respectively. As

***Table 5.*** $^{57}$Fe Mössbauer Fitting Parameters at 80 K for Selected Complexes

| cpnd | $\delta$ (mm.s$^{-1}$) | $\Delta E_Q$ (mm.s$^{-1}$) | $\lambda$ (mm.s$^{-1}$) | refs |
|---|---|---|---|---|
| {[Fe]C≡C−$(C_6H_4)_2$−C≡C[Fe]} (**5**) | 0.255 | 1.985 | 0.134 | this work |
| {[Fe]C≡C−$(C_6H_4)_2$−C≡C[Fe]}[$PF_6$]$_2$ (**5**[$PF_6$]$_2$) | 0.257 | 0.894 | 0.203 | this work |
| [[Fe]C≡C−$C_6H_4$−$C_6H_5$] (**6**) | 0.275 | 2.029 | 0.133 | this work |
| [[Fe]C≡C−$C_6H_4$−$C_6H_5$]$^+$ (**6**[$PF_6$]) | 0.256 | 0.898 | 0.118 | this work |
| [[Fe]C≡C−$C_6H_5$] (**4**) | 0.28 | 2.02 | n.r.[a] | 34 |
| [[Fe]C≡C−$C_6H_5$]$^+$ (**4**[$PF_6$]) | 0.25 | 0.90 | n.r.[a] | 34 |
| [Fe]C≡C−$C_6H_4$−C≡C[Fe] (**3**)[b] | 0.265 | 2.020 | / | 24 |
| {[Fe]C≡C−$C_6H_4$−C≡C[Fe]}$^{2+}$(**3**[$PF_6$]$_2$)[b] | 0.239 | 0.911 | / | 24 |

[a] Not reported. [b] Value recorded at 78 K.

***Table 6.*** Near-IR Data for Selected Fe(III) Complexes in $CH_2Cl_2$

| cpnd | absorptions[a] in $cm^{-1}$ ($\epsilon$[b] in $M^{-1}$ $cm^{-1}$) | $\nu_{1/2}$ ($cm^{-1}$)[c] | ref |
|---|---|---|---|
| $\{[Fe]C\equiv C-(C_6H_4)_2-C\equiv C[Fe]\}^{2+}$ ($\mathbf{5}^{2+}$) | 5450 (130) | 1400 | this work |
| $[[Fe]C\equiv C-C_6H_4-C_6H_5]^{+}$ ($\mathbf{6}^{+}$) | 5550 (80) | 1500 | this work |
| $\{[Fe]C\equiv C-C_6H_4-C\equiv C[Fe]\}^{2+}$ ($\mathbf{3}^{2+}$) | 5500 (45) | 1580 | this work |
| $\{[Fe]C\equiv CPh\}^{+}$ ($\mathbf{4}^{+}$) | 5417 (94) | 1500 | 27 |

[Fe] ≡ ($\eta^2$-dppe)($\eta^5$-$C_5Me_5$)Fe. [a] Values ± 50 $cm^{-1}$. [b] Values ± 10 $M^{-1}cm^{-1}$. [c] Values ± 200 $cm^{-1}$.

***Table 7.*** Crystal Data, Data Collection, and Refinement Parameters for **5**, **5**$[PF_6]_2$, **6**, and **6**[TCNQ]

| cpnd | 1.5(**5**)·2/3($C_4H_8O$)·1/2($C_5H_{12}$) | **5**$[PF_6]_2$·2($CH_2Cl_2$) | **6** | **6**[TCNQ]·1/4($CH_2Cl_2$) |
|---|---|---|---|---|
| formula | $C_{140.50}H_{147}Fe_3O_{1.50}P_6$ | $C_{90}H_{90}Cl_4F_{12}Fe_2P_6$ | $C_{50}H_{48}P_2Fe_1$ | $C_{62.25}H_{48.5}N_4P_2Cl_{0.5}Fe_1$, |
| fw | 2212.95 | 1838.94 | 766.67 | 992.10 |
| temp (K) | 120(1) | 120(1) | 293(2) | 120(1) |
| cryst. syst. | triclinic | triclinic | triclinic | triclinic |
| space group | P-1 | P-1 | P-1 | P-1 |
| *a* (Å) | 13.5647(3) | 10.4160(2) | 14.7336(3) | 11.1235(3) |
| *b* (Å) | 15.8974(3) | 14.1614(2) | 16.8011(3) | 11.9397(3) |
| *c* (Å) | 27.9560(4) | 15.0200(2) | 17.9380(3) | 20.8638(6) |
| α (deg) | 88.863(1) | 98.182(1) | 86.810(1) | 98.742(2) |
| $\beta$ (deg) | 78.054(1) | 99.956(1) | 67.920(1) | 95.508(2) |
| $\gamma$ (deg) | 79.310(1) | 103.838(1) | 82.818(1) | 98.512(2) |
| V($Å^3$) | 5694.5(2) | 2079.4(1) | 4082.3(1) | 2688.6 |
| Z | 2 | 1 | 4 | 2 |
| $D_{(calcd)}$ (g $cm^{-3}$) | 1.268 | 1.469 | 1.247 | 1.225 |
| crystal size (mm) | 0.22 × 0.16 × 0.1 | 0.32 × 0.28 × 0.18 | 0.32 × 0.22 × 0.20 | 0.30 × 0.30 × 0.08 |
| F(000) | 2340 | 948 | 1616 | 1037 |
| diffractometer | KappaCCD (Nonius) | KappaCCD (Nonius) | KappaCCD (Nonius) | KappaCCD (Nonius) |
| radiation | $MoK_\alpha$ | $MoK_\alpha$ | $MoK_\alpha$ | $MoK_\alpha$ |
| abs. coef. ($mm^{-1}$) | 0.507 | 0.667 | 0.482 | 0.407 |
| data collection: $\theta_{max}$ (°), | 27.2, | 27.0, | 27.0, | 27.0, |
| frames, Ω rotation (°), | 10, | 10, | 280, | 342, |
| seconds/frame | 1.0, 10 | 2.0, 30 | 2.0, 120 | 1.2, 40 |
| Θ range | 2.57−26.00 | 1.40−26.00 | 2.35−26.73 | 2.42−27.57 |
| h k l range | 0/16 −19/19 −33/34 | 0/12 −17/16 −18/17 | 0/18 −20/21 −20/22 | 0/14 −15/15 −27/26 |
| number total refl. | 79572 | 55632 | 92577 | 47838 |
| number unique refl. | 22683 | 8158 | 17314 | 12379 |
| number obs. refl. [$I > 2\sigma(I)$] | 16000 | 7276 | 11822 | 8666 |
| restraints/parameters | 0/1373 | 514 | 0/956 | 0/650 |
| $w = 1/[\sigma^2(F_o)^2+(aP)^2+bP]$ (where $P = [F_o^2+F_c^2]/3$) | $a = 0.1127$ $b = 9.5157$ | $a = 0.0652$ $b = 2.2205$ | $a = 0.0783$ $b = 1.0811$ | $a = 0.0806$ $b = 2.6631$ |
| final *R* | 0.068 | 0.042 | 0.048 | 0.060 |
| $R_w$ | 0.186 | 0.115 | 0.123 | 0.149 |
| *R* indices (all data) | 0.104 | 0.048 | 0.083 | 0.098 |
| $R_w$ (all data) | 0.215 | 0.122 | 0.148 | 0.172 |
| goodness of fit/$F^2$ ($S_w$) | 1.087 | 1.101 | 1.017 | 1.025 |
| $\Delta\rho_{max}$ (e $Å^{-3}$) | 1.168 | 0.819 | 0.373 | 0.922 |
| $\Delta\rho_{min}$ (e $Å^{-3}$) | −0.889 | −0.573 | −0.370 | −0.510 |

mentioned above, the bond lengths and angles compare with those of **5** and **5**$[PF_6]_2$ (See Supporting Information), and are also in good accordance with crystallographic data available for related mononuclear Fe(II) and Fe(III) compounds.[23,26,27] The changes in the coordination sphere occurring upon oxidation have been discussed in detail elsewhere.[26,27] The two aryl rings in the biphenyl moiety are tilted from an angle of ca. 30°, regardless of the oxidation state of the metal center, suggesting that the latter has only a negligible electronic influence on this angle in **6**/**6**$^+$. The geometric features of the TCNQ counterion in **6**[TCNQ] are also quite usual, a slight dissymmetry being observed between the cyano bonds on opposite exocyclic carbon atoms on the central ring, which can be imparted to a weak stacking $\pi$-interaction taking place (distance C57−C57 = 3.186 Å) between TCNQ pairs in the elementary cell. Apart from that, no specific intermolecular interaction takes place and a dichloromethane solvate partially occupies the voids between molecules in **6**[TCNQ].

**Generation and Characterization of the Mixed Valence Complex 5$^+$.** The mixed valence (MV) complex **5**$^+$ has been

(38) Ovchinnikov, A. O. *Theor. Chim. Acta (Berl.)* **1978**, *47*, 297−304.
(39) (a) Kahn, O. *Molecular Magnetism*; VCH Publisher Inc.: New York Weinheim Cambridge, 1993. (b) Evans, D. F. *J. Chem. Soc.* **1959**, 2003−2004. (c) Schubert, E. M. *J. Chem. Educ.* **1992**, *69*, 62.
(40) Le Narvor, N.; Lapinte, C. *C. R. Acad. Sci., T. 1, Ser. IIc* **1998**, 745−749.
(41) Le Stang, S.; Paul, F.; Lapinte, C. *Inorg. Chim. Acta* **1999**, *291*, 403−425.
(42) (a) Lemée, M. H.; Toupet, L.; Délugeard, Y.; Messager, J. C.; Cailleau, H. *Acta Crystallogr.* **1987**, *B43*, 446−470. (b) Saito, K.; Atake, T.; Chihara, H. *Acta Crystallogr.* **1987**, *B43*, 383−385. (c) One referee suggested that apparent planarity could result from rapid interconversion between slightly twisted conformations (see Baudour; J.-L. *Acta Crystallogr.* **1991**, *B47*, 935−949 for details). Presently, the anisotropic refinements reveal nothing unusual, as expected for a truly planar biphenyl unit in the solid state.

***Table 8.*** Near-IR Data for Selected **5**[$PF_6$] and **3**[$PF_6$] in $CH_2Cl_2$

| cpnd | band | $\nu_{max}$ in $cm^{-1}$ ($\epsilon$ in $M^{-1}$ $cm^{-1}$)[a] | $(\nu_{1/2})_{exp}$ ($cm^{-1}$)[b] | $d_{ab}$ (Å)[c] | $(\nu_{1/2})_{theo}$ ($cm^{-1}$)[d] | $H_{ab}$ ($cm^{-1}$) |
|---|---|---|---|---|---|---|
| [Fe]C≡C−($C_6H_4$)$_2$−C≡C[Fe]$^+$ (**5**$^+$) | B | 5000 (240) | 1650 | 16.1 | 3381 | / |
| | | 5250 (290)[e] | 1650[e] | | 3480[e] | / |
| | | 5500 (160)[f] | 1650[f] | | 3565[f] | / |
| | C | 6250 (560) | 3750 | 16.1 | 3800 | 145[g] |
| | | 7090 (660)[e] | 4050[e] | | 4050[e] | 176[e,g] |
| | | 7350 (625)[f] | 4410[f] | | 4120[f] | 182[f,g] |
| [Fe]C≡C−$C_6H_4$−C≡C[Fe]$^+$ (**3**$^+$) | A | 4000 (12700) | 2120 | 11.6 | 3040 | 590[g] |
| | | | | | | 2000[h] |
| | B | 6500 (3400) | 2110 | / | 3880 | / |
| | C | 9000 (600) | 2110 | / | 4560 | / |
| | D | 5400 (300) | 1580 | / | 3530 | / |

[Fe] ≡ ($\eta^2$-dppe)($\eta^5$-$C_5Me_5$)Fe. [a] Values ± 10 $M^{-1}cm^{-1}$. [b] Values ± 50 $cm^{-1}$. [c] Evaluated from X-ray structures or calculated from DFT. [d] Calculated following eq 4. [e] In dichloromethane/acetone (1:1) mixture. [f] In neat acetone. [g] Calculated following eq 3. [h] Calculated following eq 11.

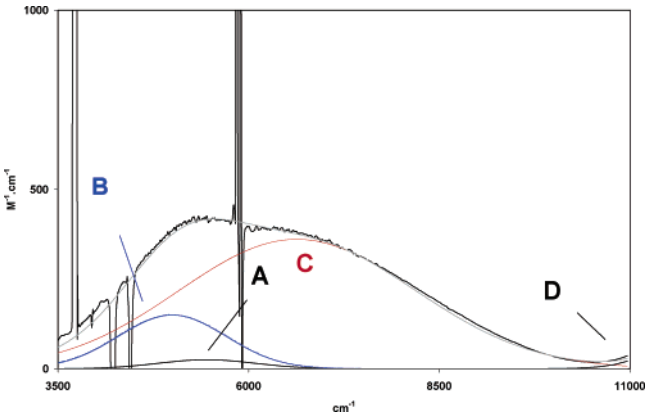


***Figure 8.*** Near-IR spectra for an equimolar mixture of **5** (2 $10^{-3}$ M) and **5**[$PF_6$]$_2$ (2 $10^{-3}$ M) in dichloromethane and proposed de-convolution.

generated following the comproportionation reaction given in eq 1, by mixing equimolar amounts of **5** and **5**$^{2+}$. However, the electrochemical data reveals that **5**$^+$ is not sufficiently stable to exist in solution as a single product within this equilibrium. Thus, once generated in solution, it will equilibrate with ca. 18% of **5** and 18% of **5**$^{2+}$, and the occurrence of these two species has to be taken into consideration during the ensuing spectroscopic studies.

From these solutions, two new infrared bands could be detected in the acetylide stretching region which presumably correspond to the MV complex at 2043 and 1979 $cm^{-1}$ (Table 1 and Figure 1). Also, after thawing a solution containing equimolar mixtures of **5** and **5**[$PF_6$]$_2$, a new rhombic signal can be detected by ESR in addition to the signal of the diradical **5**[$PF_6$]$_2$, with main $g$-components at $g_1 = 1.976$, $g_2 = 2.134$ and $g_3 = 2.418$ (Table 4). This signal resembles that observed for **6**[$PF_6$] ($g_1 = 1.975$, $g_2 = 2.032$, and $g_3 = 2.439$) and is typical of an Fe(III)-centered radical in cationic piano-stool acetylide complexes.[27] The anisotropy of the signal is also very close to that previously observed for related mononuclear complexes such as **6**[$PF_6$] or **4**[$PF_6$] (Figure 7 and Table 4). Finally, in the near-IR range a new broad absorption centered at ca. 6500 $cm^{-1}$ shows up which is not present in solutions of pure **5** or **5**[$PF_6$]$_2$ complexes. De-convolution of the spectrum in this spectral range using Gaussian functions reveals the presence of two new overlapping transitions attributable to **5**$^+$ in addition to the weak transition (A) at 5450 $cm^{-1}$ expected for **5**$^{2+}$ in equilibrium with **5**$^+$ (Figure 8 and Table 8). The onset of a band (D) which corresponds to the strong absorptions in the visible range at ca. 726 nm for both **5**$^+$ and **5**$^{2+}$complexes

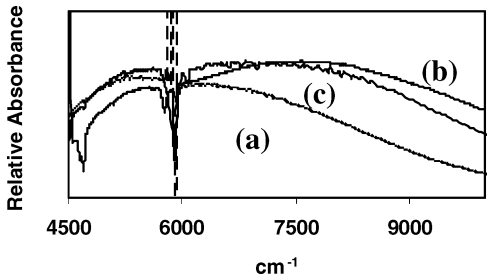


***Figure 9.*** Near-IR spectra for mixtures of **5**/**5**[$PF_6$]$_2$ in dichloromethane (a), in acetone (b) and in a 1:1 mixture of both solvents (c).

(Table 2) has also been introduced in the deconvolution. Among the new bands detected, the first one (B) at 5000 $cm^{-1}$ is rather weak while the second one (C) at 6250 $cm^{-1}$ is significantly more intense. The former is attributed to a ligand field (LF) transition, also called interconfigurational (IC) transition by Demadis et al.,[10] by analogy with the absorptions previously detected in related Fe(III) aryl acetylides.[27] This transition is red-shifted of ca. 450 $cm^{-1}$ relative to similar processes occurring at 5450 $cm^{-1}$ for **5**$^{2+}$ and at 5417 and 5500 $cm^{-1}$ for the mononuclear complexes **4**$^+$ or **6**$^+$ respectively (Table 8). The band (C) in Figure 8 is believed to correspond to an intervalence charge-transfer transition (IVCT). Its width at half-height $(\nu_{1/2})_{exp}$, is well in line with predictions based on the Hush model ($(\nu_{1/2})_{theo}$ in Table 8).[14b,16a,43] Notably, band B is much narrower than predicted on the basis of eq 4 and presents an experimental $\nu_{1/2}$ in the range usually observed for such transitions.[27]

The influence of the solvent polarity on these bands was also briefly investigated. However, due to the low solubility of **5** in common polar solvents, the use of such solvents resulted in the rapid precipitation of this complex, driving the comproportionation equilibrium (eq 1) toward the left. Among the polar solvents tested, only acetone proved suitable to this experiment, since the precipitation of **5** in neat acetone occurred much more slowly (after 10 mn) and the measurements could be performed directly after dissolution. While remaining essentially qualitative in neat acetone, the data obtained from dichloromethane, acetone and a 1:1 mixture of these solvents clearly establish a solvatochromic behavior for the band envelope of the broad near-IR absorption (Figure 9). Spectral data extracted from these experiments (Table 8) reveals that both Gaussian bands B and C are shifted toward higher energies when the polarity of the

(43) The so-called "semiclassical" treatment has been used to deconvolute this band.[16a]

medium increases, but that band C is much more strongly affected by this change than is band B. Notably, there is also a concomitant increase in band C bandwidth when it shifts to higher energy, as expected for an IVCT process following the Hush model (equations 3 and 4). In contrast, despite the slight shift of band B its bandwidth does apparently not change, further confirming that this transition has nothing to do with an IVCT process. Note, however, that the bandwidth found for **5**[$PF_6$] in neat acetone is larger than theoretically expected on the basis of eq 3. In the absence of identified causes for additional line broadening, this might be attributed to the experimental uncertainties associated with this measurement. Finally, there is also an apparent enhancement in the relative intensity of band C in the more polar media tested.

$$H_{ab} = (2.06 \times 10^{-2}/d_{ab})(\epsilon_{max}\, \nu_{max}\, \Delta\nu_{1/2})^{1/2} \qquad (3)$$

$$(\nu_{1/2})_{theo} = (2310.\nu_{max})^{1/2} \qquad (4)$$

**Study of the Near-IR Absorptions of the Mixed Valence Complex $3^+$.** For comparison purposes, we have also recorded the near-IR spectra of the MV dinuclear complex **3**[$PF_6$] under similar conditions, synthesized as previously described.[24] This time, the MV complex can be considered as being the only species in solution ($K_c = 2.6\ 10^4$) according to an equilibrium similar to that given in eq 1. A strong near-IR absorption is observed which obviously corresponds to an overlay of several peaks. It is much stronger than that observed for **5**[$PF_6$] and presents an apparent maximum at lower energy (ca. 4340 $cm^{-1}$).[44] We verified that this strong near-IR-absorption is specific to **3**[$PF_6$]. Thus, this feature disappears upon oxidation or reduction and we have verified that it can be obtained either from the isolated MV complex **3**[$PF_6$] or from **3**[$PF_6$] generated in situ by comproportionation of **3** and **3**[$PF_6$]$_2$.

De-convolution of the near-IR absorption in Gaussian sub-bands proved less straightforward than for **5**[$PF_6$]. Indeed, correct fits can be obtained in different ways. For instance, the observed spectrum can be fitted with a single transition presenting a partly resolved vibronic progression (see Supporting Information).[45] To the best of our knowledge, vibronic progressions observed so far on IVCTs involved fewer vibronic sub-bands than needed here.[11,46] Moreover, such vibronic progressions on the IVCT band were observed only for fully delocalized (class-III) MV compounds, and **3**[$PF_6$] is not a fully delocalized MV complex (see below).

Alternatively, the de-convolution of the near-IR spectrum of **3**[$PF_6$] can be attempted using distinct overlapping transitions. Meyer and co-workers[10] have conclusively shown that inorganic

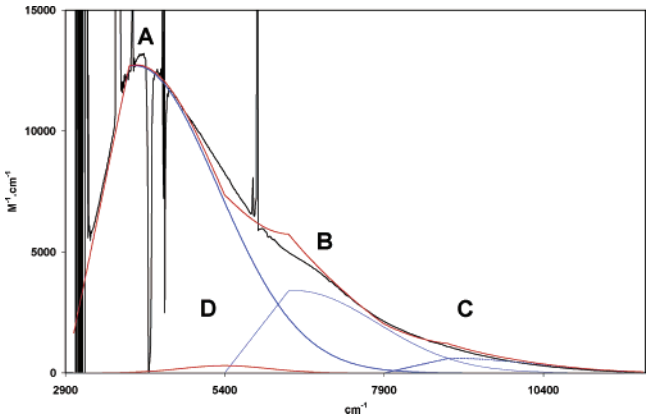


***Figure 10.*** Near-IR spectra for **3**[$PF_6$] (2 $10^{-4}$ M) in dichloromethane and proposed deconvolution.

MV complexes possessing several electrons on metal d sublevels in pseudo-octahedral environments might give rise to three optical electron-transfer processes when the metal−metal interaction mediated by the bridging ligand is strong and when these levels lie close in energy to the SOMO/SOMO-1 levels which usually give rise to the lowest-energy intervalence transfer process.[47] Multiple optical electron-transfer processes were also recently envisioned by Sponsler and co-workers as possible sources of sidebands for related dinuclear MV complexes presenting related IVCT bands.[48] This is indeed particularly true for MV complexes containing "($\eta^2$-dppe)($\eta^5$-$C_5Me_5$)Fe" end-groups, since the SOMO-2 to SOMO-4 are largely metal-centered with respectively strong $d_{xz}$ and $d_{x2-y2}$ character and usually lie quite close in energy to the SOMO/SOMO-1 levels which presents a strong $d_{yz}$ character (the *z*-axis being defined along the Fe−Fe axis, with the *y*-axis pointing toward the permethylated cyclopentadienyl ligand).[27] We presently checked this possibility, and the de-convolution of the near-IR-absorption was attempted using the minimum number of sub-bands to accurately fit the spectrum, starting from its most intense part.[49] Since no bridge-centered oxidation is expected for **3**[$PF_6$] in the ground state (GS) based on previous characterizations,[24] the lowest-energy allowed transition (A) was considered to correspond to the "normal" metal−metal optical electron-transfer (IVCT). Consequently, the first sub-band (A) at 4000 $cm^{-1}$ was then supposed to obey the two-level model and to exhibit a half-width ($\nu_{1/2}$) corresponding to eq 4. A half-width of 3040 $cm^{-1}$ was therefore used for this curve. However, such a Gaussian sub-band cannot fit the low-energy side of the spectrum (Figure 10) and has to be truncated. This is not surprising since similar cutoffs are often observed with strongly coupled MV complexes when the electronic coupling ($H_{ab}$) becomes close to half of the reorganization energy ($\lambda/2$).[11,16a,47] Accordingly, we have truncated this first sub-band using a

(44) Notably, the apparent absorption maximum is roughly twice as intense (ca. 13300 vs 5940 $M^{-1}cm^{-1}$) and located at a lower energy (ca. 4120 vs 4960 $cm^{-1}$) than reported previously with a sample of **3**[$PF_6$].[8a] We believe that this is due to the poor sensitivity of the spectrometer previously used in this spectral range.

(45) In line with the recent contribution of Bailey and co-workers,[46] the spectrum can be fitted using a series of Gaussian curves of decreasing intensity (see Supporting Information); the main peak would be at 3950 $cm^{-1}$ with a vibronic progression of ca. 1000 $cm^{-1}$, each sub-band exhibiting a significantly smaller half-width than expected based on Hush model (ca. 1200 $cm^{-1}$). Presently, this progression could have corresponded to a strong infrared-active mode observed at 1020 $cm^{-1}$ in **3**[$PF_6$]. Note however that such a correspondence is not required given the existence of "missing mode effects" (MIME).[46] Note also that other vibronic deconvolutions can be obtained, especially when using less energetic progressions.

(46) Bailey, S. E.; Zink, J. I.; Nelsen, S. F. *J. Am. Chem. Soc.* **2003**, *125*, 5939−5947.

(47) Al-Noami, M.; Yap, G. P. A.; Crutchley, R. J. *Inorg. Chem.* **2004**, *43*, 1770−1778.

(48) Chung, M.-I.; Gu, X.; Etzenhouser, B. A.; Spuches, A. M.; Rye, P. T.; Seetharaman, S. K.; Rose, D. J.; Zubieta, J.; Sponsler, M. B. *Organometallics* **2003**, *22*, 3485−3494.

(49) An electron-transfer process (LMCT) to form an excited state with a bridge-localized oxidation could also be envisioned with **3**[$PF_6$] to rationalize one of the observed bands (B or C). Such processes were recently demonstrated to occur in strongly coupled organic MV complexes featuring phenylene bridges and produce very similar band shapes in the near-IR domain, when not fully resolved.[50] While such an explanation cannot yet be disregarded, we favour the former hypothesis, since MLCT processes occur usually above 14 000 $cm^{-1}$ in mononuclear model complexes and are believed to be also observed in this region with **3**[$PF_6$] (Table 2) based on DFT computations.[19]

straight line in order to obtain the better fit of the low-energy side. As seen in Figure 10, the truncation of the real spectrum occurs more progressively certainly due to quantum effects "rounding off the corners".[11] At this stage, the fit can be completed with two additional sub-bands, B and C, at 6500 and 9000 $cm^{-1}$, respectively, presenting the same half-width and cutoff as band A (B and C; see Table 8 for details). In line with Meyer's proposal, this implies that these sub-bands correspond to IVCT processes with comparable reorganization energies to that of band A. Furthermore, in such a case, the energies of the three optical metal−metal electron transfers ($E_{IVCT}(1) - E_{IVCT}(3)$) are roughly related to the energies of two LF transitions $E_{LF}(1)$ and $E_{LF}(2)$ by eqs 5−7.[10] According to eqs 5−7 and to the values found for $E_{IVCT}(2)$ and $E_{IVCT}(3)$ (Table 8), the energies of these LF transitions should take place at ca. 2500 and 5000 $cm^{-1}$, which is in line with independent estimates of these processes.[27] Unfortunately, the high intensities of sub-bands A and B preclude the detection of the "forbidden" LF(2) transition at 5000 $cm^{-1}$ on the experimental spectrum with confidence, while the other "forbidden" transition (LF(1)) lies outside the spectrometer range. Nevertheless, it is apparent that the use of an additional weak sub-band (D) at ca. 5400 $cm^{-1}$ does significantly improve the fit (Figure 10). While the fit obtained with these four sub-bands (A−D) is evidently quite approximate in comparison with the real spectrum, we consider it to be satisfactory in regard to the various approximations made (notably the similar reorganization energies and linear cutoff used for sub-bands A−C).

$$E_{IVCT}(1) \approx \lambda \quad (5)$$

$$E_{IVCT}(2) \approx \lambda + E_{LF}(1) \quad (6)$$

$$E_{IVCT}(3) \approx \lambda + E_{LF}(2) \quad (7)$$

Regardless which deconvolution is considered, the strong intensity of the near-IR absorption reveals a rather large transition moment for **3**[$PF_6$] which, in turn, implies a strongly allowed (IVCT) process corresponding to a strongly coupled MV complex. In line with this hypothesis, the near-IR spectrum is only marginally affected by a change in the solvent polarity (see Supporting Information). As for **5**[$PF_6$] (see above), the very low solubility of the neutral complex (**3**) in common solvents restricted us to the use of a few dichloromethane-solvent mixtures for this investigation.

**Electronic Delocalization in the Mixed Valence Complex $5^+$ versus $3^+$.** The observation of two $\nu_{C\equiv C}$ for the MV complex $5^+$, while only one had previously been detected for both **5** and $5^{2+}$ evidences a localization of the valence at the time scale of the infrared spectrometry (ca. $10^{-12}$ s) and strongly suggests that we are not dealing here with a class-III MV complex.[15,16a] In line with this observation, the electronic spectrum of $5^+$ in the UV−vis range is merely a superposition of the absorption observed for **5** and $5^{2+}$ (Figure 4). While the detection of an IVCT band in the near-IR domain indicate that **5**[$PF_6$] is not a class-I MV compound, the negative solvatochromic behavior evidenced for the IVCT band (Figure 9) establishes **5**[$PF_6$] as a class-II MV complex. Notably, this shift to higher energies for more polar solvents and the simultaneous increase in half-width conforming to eq 4 is exactly what is expected for a weakly coupled MV complex or class-IIA complex.[14b,16a] This is also consistent with the Γ parameter determined according to eqs 8 and 9.[16a] The later (Γ = 0.013) gives also a measure of the degree of delocalization of the unpaired electron in **5**[$PF_6$].

$$\Gamma = (1\text{-}\theta) \quad (8)$$

$$\theta = (\nu_{1/2})_{exp}/(2310.\nu_{max})^{1/2} \quad (9)$$

The electronic coupling derived for this complex (eq 5) proves quite sizable for two metal centers situated 16 Å apart.[5,10−13] The significant improvement in the electronic coupling (+25%) found for **5**[$PF_6$] in acetone is quite surprising and should be considered with caution given the experimental uncertainties associated with the detection of weak IVCT bands and the poor solubility of **5** in this solvent (see above).[51] In the absence of additional data, one could also tentatively relate this observation to a solvent-induced increase of the comproportionation constant ($K_c$ in eq 1) in more polar media resulting in an apparent increase of the IVCT band. More interestingly, the unambiguous class-II categorization of **5**[$PF_6$] means that the $\nu_{max}$ experimentally found for band B (6250 $cm^{-1}$) corresponds to the reorganization energy ($\lambda$) of the optical electron-transfer process. Given its relative magnitude in comparison to the electronic coupling ($2H_{ab}/\lambda = 0.046$), no cutoff of the IVCT band is expected, as observed.

While the valency seems localized at IR time scales ($10^{-12}$ s), the ESR signal obtained for **5**[$PF_6$] is quite typical of a single Fe(III) center and shows only a slightly diminished anisotropy ($\Delta g = 0.442$) in comparison to the mononuclear complex **6**[$PF_6$] ($\Delta g = 0.464$). This slight change could actually be induced by the electronic exchange process between metal centers, since the rate of electron transfer ($k_{ET}$) is calculated to be around 5 $10^9$ $s^{-1}$ at 300 K using eq 10 (nonadiabatic electron transfer) for a weakly coupled MV complex (see below).[16a,53] Whatever the rate of the exchange, the ESR data unambiguously shows that the unpaired electron is dominantly metal-centered, further emphasizing a class-II categorization for **5**[$PF_6$].

$$[2\,(H_{ab})^2/h][\pi^3/\lambda RT]^{1/2}\exp[-(\lambda - 2H_{ab})^2/(4\lambda RT)] \quad (10)$$

$$H_{ab} = (\nu_{max})/2 \quad (11)$$

While the data for **5**[$PF_6$] are in accordance with a mixed-valent (MV) complex presenting a localized valency, the data for $3^+$ is strongly reminiscent of that recently obtained with $2^+$ (Chart 1), proposed to be a Class-IIIA MV complex.[16a,19] Accordingly, the high intensity of the near-IR (IVCT) transition and its distinctly truncated shape on the low-energy side is suggestive of a strongly coupled MV complex.[11,46−47,54,55] However, **3**[$PF_6$] is not fully delocalized (class-III) at the time scale of the molecular vibrations ($10^{-13}$ s) since two $\nu_{C\equiv C}$ modes are observed in solution and in the solid state (KBr pellets), in line with an overall dissymmetric structure (i.e., partly localized valency) at ambient temperatures.[24] As previously supposed,[8a]

(50) Lambert, C.; Amthor, S.; Schelter, J. *J. Phys. Chem.* **2004**, *108*, 6474−6486.
(51) Note that solvent-dependent electronic couplings have been occasionally reported for organic[52] or inorganic[47] MV compounds.
(52) Nelsen, S. F.; Konradsson, A. E.; Telo, J. P. *J. Am. Chem. Soc.* **2005**, *127*, 920−925.
(53) A very similar result is also obtained when the corresponding equation for an adiabatic electron transfer is considered, with a nuclear factor of $5 \times 10^{12}$ $s^{-1}$.

**3**[$PF_6$] must belong to the class-IIB and therefore constitutes a limiting case between class-II and class-III with ($H_{ab} \leq \lambda/2$).[16a] The reorganization energy for the optical electron transfer of lowest energy (A) in this complex is given by $\nu_{max}$ ($\lambda_{eff} = 4000$ $cm^{-1}$). It is lower than that for **5**[$PF_6$] ($\lambda = 6250$ $cm^{-1}$), as expected when going to a more delocalized and shorter MV complex like **3**[$PF_6$]. An electronic coupling of 1700 $cm^{-1}$ and a $\Gamma$ parameter of 0.30 can be derived from the experimental bandwidth (equation 12), which implies a significantly larger electronic delocalization than in **5**[$PF_6$].[56,57] In line with the negligible solvatochromy of band (A), the electronic coupling is close to the higher limit of $H_{ab}$ derived in Table 8 (452 $cm^{-1} < H_{ab} < 2000$ $cm^{-1}$). This value also suggest a diminished electronic delocalization relative to the 9,10-anthryl analogue **2**[$PF_6$], as was to be expected from published data.[58,59]

$$\Gamma = 1/2 - (\lambda - 2H_{ab})/(\nu_{1/2})_{theo} \qquad (12)$$

## Conclusions

In this contribution, we have reported on the synthesis and characterization of a new family of binuclear acetylide complexes featuring electron-rich "($\eta^2$-dppe)($\eta^5$-$C_5Me_5$)Fe(C≡C)" endgroups with a 4,4′-biphenyl spacer inserted in the carbon-rich bridge. Although no splitting of the Fe(III/II) redox wave was discernible in the cyclic voltammogram, the comproportionation constant of **5**[$PF_6$] could be measured by cyclic voltammetry (Kc around 10). With such a low value, the selective isolation of the MV complex **5**[$PF_6$] proved not possible, but the latter could be characterized in solution by various spectrometries. An IVCT band was detected in the near-IR domain, evidencing the existence of a photodriven metal−metal electron-transfer process between metal centers ca. 16 Å apart. The reorganization energy of this intramolecular process amounts to ca. 6250 $cm^{-1}$ in dichloromethane and an electronic coupling of ca. 150 $cm^{-1}$ could also be derived for this process.[60] Notably, this study reveals that **5**[$PF_6$] constitutes an(other) example of well behaved weakly coupled class-IIA organometallic MV compound according to the Robin and Day classification and, considering the high consistency of the experimental data gathered for this compound, justifies a posteriori the use of a two-level model to interpret the experimental data. The near-IR absorption of the known and much more stable MV analogue **3**[$PF_6$] presenting the 1,4-phenyl unit instead of the 4,4′-biphenyl one ($K_c = 2.6\ 10^4$) was also closely reexamined. We consider it as mainly resulting from the overlap of three optical electron-transfer processes involving lower lying d electrons. Under such an assumption, an electronic coupling of ca. 1700 $cm^{-1}$ can be derived from the band shape for this MV complex in the frame of the two-level model. Whatever the assignments made, the redox centers are more strongly coupled in this second compound, which lies much closer to the borderline between class-II and class-III than **5**[$PF_6$]. Consequently, this work clearly demonstrates that the electron exchange is not dramatically depressed by insertion of a second *para*-phenylene moiety into a 1,4-dietynylaryl bridge, but simply slowed, as expected when going from **3**[$PF_6$] to **5**[$PF_6$]. Thus, the successive insertion of 1,4-phenylene units in the middle of the butadiyne-diyl bridge of the Class-IIIA MV complex **1a**[$PF_6$] results in a progressive transition toward a Class-IIA (**5**[$PF_6$]) MV complex, via a Class-IIB (**3**[$PF_6$]) MV complex.

## Experimental Section

**General Data.** All manipulations were carried out under inert atmospheres. Solvents or reagents were used as follows: $Et_2O$ and *n*-pentane, distilled from Na/benzophenone; $CH_2Cl_2$, distilled from $CaH_2$ and purged with argon; $HN(^iPr)_2$, distilled from KOH and purged with argon; aryl bromides (Acros, >99%), opened/stored under Ar. The [($\eta^5$-$C_5H_5)_2$Fe][$PF_6$] ferricinium salt was prepared by previously published procedures.[33] Transmittance-FTIR spectra were recorded using a Bruker IFS28 spectrometer (400−4000 $cm^{-1}$). Raman spectra of the solid samples were obtained by diffuse scattering on the same appartus and recorded in the 100−3300 $cm^{-1}$ range (Stokes emission) with a laser excitation source at 1064 nm (25 mW) and a quartz separator with a FRA 106 detector. Near-IR (near-IR) spectra were recorded using a Bruker IFS28 spectrometer, using a Nernst Globar source and a KBr separator with a DTGS detector (400−7500 $cm^{-1}$) or tungsten source and a quartz separator with a Peltier-effect detector (5200−12500 $cm^{-1}$) or on a Cary 5 spectrometer. UV−Visible spectra were recorded on an UVIKON XL spectrometer. ESR spectra were recorded on a Bruker EMX-8/2.7 (X-band) spectrometer. Elemental analyses were performed at the "Centre Regional de Mesures Physiques de l'Ouest" (C. R. M. P. O., University of Rennes).

**Synthesis of the Binuclear Bis-vinylidene Fe(II) complex [{($\eta^2$-dppe)($\eta^5$-$C_5Me_5$)Fe}$_2$(=C=CH-4,4′-{1,1′-($C_6H_4$)$_2$}−HC=C=)][$BPh_4$]$_2$ (5v[$BPh_4$]$_2$).** In a Schlenk tube, 0.50 g of 4,4′-bis-ethynyl-2,2′-biphenyl (2.47 mmol), 3.08 g of ($\eta^2$-dppe)($\eta^5$-$C_5Me_5$)FeCl (4.94 mmol) and 1.80 g of [Na][$BPh_4$] (5.26 mmol) were introduced under argon. A mixture of MeOH/THF (30/10 mL) was added and the dark green suspension was stirred for 32 h. The solvent was then removed in vacuo and the residue was extracted with $CH_2C1_2$. The extract was concentrated and *n*-pentane was added to precipitate the [{($\eta^2$-dppe)($\eta^5$-$C_5Me_5$)Fe}$_2$(=C=CH-1,4-{1,1′-($C_6H_4$)$_2$}−HC=C=)][$BPh_4$]$_2$ vinylidene complex (**5v**[$BPh_4$]$_2$) as a pale brown powder which was subsequently washed with diethyl ether and dried in vacuo. Yield 80%. FT-IR (KBr, $\nu$ in $cm^{-1}$) 1616 (m, Fe=C=C). $^{31}$P NMR (81 MHz, $CDCl_3$, $\delta$ in ppm) 88.5 (s, 2 P, dppe). $^1$H NMR (200 MHz, $CDCl_3$, $\delta$ in ppm) 7.70−6.75 (m, 84 H, $H_{Ar}$); 6.42 (d, 4 H, $^4J_{PH} = 8.2$ Hz, $H_{Ar}$); 5.18 (t, 2 H, $^4J_{PH} = 4.6$ Hz, C=C*H*); 2.25−2.85 (2m, 8 H, P$CH_2$); 1.30 (s, 30 H, $C_5Me_5$). $^{13}$C NMR (50 MHz, $CDCl_3$, $\delta$ in ppm) 363.4 (t, $^2J_{CP} = 27$ Hz, Fe=*C*=C); 164.6 (q, $^1J_{BC} = 50$ Hz, B−$C_{Ar}$); 135.7−125.7 (12 s, $C_{Ar}$); 136.8, 125.9, 122.1 (s, $C_{Ar(BPh4)}$), 126.4 (s, Fe=C=*C*H); 99.8 (s, $C_5Me_5$); 28.3 (m, P*C*H$_2$); 9.4 (s, $C_5$*Me*$_5$).

**Synthesis of the Binuclear Bis-alkyny1 Fe(II) Complex {($\eta^2$-dppe)($\eta^5$-$C_5Me_5$)Fe}$_2$(C≡C-4,4′-{1,1′-($C_6H_4$)$_2$}C≡C) (5).** In a Schlenk tube, 3.00 g of bis-viny1idene complex **5v**[$BPh_4$]$_2$ (1.76 mmol) and 0.40 g of $^t$BuOK (3.54 mmol) and THF were introduced under argon.

(54) Low, P. J.; Paterson, M. A. J.; Puschmann, H.; Goeta, A. E.; Howard, J. A. K.; Lambert, C.; Cherryman, J. C.; Tackley, D. R.; Leeming, S.; Brown, B. *Chem. Eur. J.* **2004**, *10*, 83−91.

(55) Szeghalmi, A. V.; Erdmann, M.; Engel, V.; Schmitt, M.; Amthor, S.; Kriegisch, V.; Nöll, G.; Stahl, R.; lambert, C.; Leusser, D.; Stalke, D.; Zabel, M.; Popp, J. *J. Am. Chem. Soc.* **2004**, *126*, 7834−7845.

(56) Although the two-level approach (equations 3−4 and 11) might constitute a poor model to accurately derive the energy of the electronic coupling for localized MV compounds when several diabatic states interact with the (degenerate) GS,[57] this approach remains correct provided that the four closely lying interconfigurational diabatic (LF) states couple only weakly with the two degenerate diabatic ground states and provided the Born−Oppenheimer approximation still holds. The first condition is certainly fulfilled for **3**[$PF_6$] considering the poor overlap and the energetical gaps between the different metal-centred frontier molecular orbitals presenting a different d character.[27]

(57) Coropceanu, V.; Malagoli, M.; André, J. M.; Brédas, J. L. *J. Am. Chem. Soc.* **2002**, *124*, 10519−10530.

(58) (a) Lambert, C.; Nöll, G.; Schelter, J. *Nat. Mater.* **2002**, *1*, 69−73. (b) Gao, L.-B.; Zhang, L.-Y.; Shi, L.-X.; Chen, Z.-N. *Organometallics* **2005**, *24*, 1678−1684. (c) Fraysse, S.; Coudret, C.; Launay, J.-P. *J. Am. Chem. Soc.* **2003**, *125*, 5880−5888.

(59) Karafiloglou, P.; Launay, J. P. *Chem. Phys.* **2003**, *289*, 231−242.

(60) As suggested by one referee, the value of 145 $cm^{-1}$ found is certainly not "unusually high" for the bridge featuring a 2,2′-biphenyl spacer. This is also indicated by the plot of the logarithm of $H_{ab}$ versus the number of bonds between the irons atoms in the series **1a**[$PF_6$], **3**[$PF_6$], and **5**[$PF_6$] which appears reasonably linear (see Supporting Information), the value for **5**[$PF_6$] being slightly below the value expected.

The dark red solution was stirred for 7 h and the solvent was removed in vacuo. The residue was extracted with toluene and the extract was concentrated, before addition of *n*-pentane to precipitate {($\eta^2$-dppe)-($\eta^5$-$C_5Me_5$)Fe}$_2$(C≡C-4,4′-{1,1′-($C_6H_4$)$_2$}C≡C) the alkynyl complex (**5**) as a red powder which was subsequently dried in vacuo. Yield 90%. Dark red crystals of **5** could be grown by (i) allowing diethyl ether to slowly diffuse into a nitrobenzene solution of the compound or (ii) by slow evaporation of a THF/*n*-pentane solution of **5**. MS (FAB$^+$, *m*-NBA) *m*/*z* 1378.4383 ([M]$^+$, 100%), *m*/*z* calcd. for [$C_{88}H_{86}P_4{}^{56}Fe_2{}^+$] = 1378.4379. Anal. Calcd. for $C_{88}H_{86}P_4Fe_2$: C, 76.63; H, 6.29. Found: C, 76.78; H, 6.53. FT-IR (KBr, $\nu$ in cm$^{-1}$) 2051 (s, C≡C); 1597 (vs, Ar($A_1$)). Raman ($\nu$, cm$^{-1}$) 2057, 2030 (vw, C≡C); 1590 (vs, Ar($A_1$)). $^{31}$P NMR (81 MHz, $CDCl_3$, $\delta$ in ppm) 101.1 (s, 2P, dppe). $^1$H NMR (500 MHz, $C_7D_8$, $\delta$ in ppm) 8.05 (m, 8 H, 4 $H_{Ar}$); 7.46 (d, $^3J_{HH}$ = 7.2 Hz, 4 H, $H_{Ar}$); 7.75−7.00 (m, 36 H, $H_{Ar}$); 2.05−2.75 (2m, 8 H, PC$H_2$); 1.47 (s, 30 H, $C_5Me_5$). $^{13}$C NMR (75 MHz, $CD_3C_6D_5$, $\delta$ in ppm) 142.3 (t, $^2J_{CP}$ = 39 Hz, Fe-*C*≡C); 140.0−120.4 (12 s, $C_{Ar}$); 120.4 (s, Fe−C≡*C*); 88.4 (s, $C_5Me_5$); 29.5 (m, P$CH_2$); 9.9 (s, $C_5Me_5$).

**Synthesis of the Binuclear Bis-alkyny1 Fe(III) Complex [{($\eta^2$-dppe)($\eta^5$-$C_5Me_5$)Fe}$_2$(C≡C-4,4′-{1,1′-($C_6H_4$)$_2$}C≡C)][$PF_6$]$_2$ (5[$PF_6$]$_2$).** To a 1.00 g suspension of the bis-alkynyl complex **5** (0.74 mmol) in 50 mL dichloromethane, 0.49 g of [Fe($\eta^5$-$C_5H_5$)$_2$][$PF_6$] (1.48 mmol) was added, resulting in an instantaneous darkening of the solution. Stirring was maintained 3 h at room temperature and the solution was concentrated in vacuo to ca. 5 mL. Addition of 50 mL of *n*-pentane allowed precipitation of a dark solid. Decantation and subsequent washing with 2 × 3 mL portions of toluene followed by 2 × 3 mL diethyl ether and drying under vacuum yielded the desired [{($\eta^2$-dppe)-($\eta^5$-$C_5Me_5$)Fe}$_2$(C≡C-4,4′-{1,1′-($C_6H_4$)$_2$}C≡C)][$PF_6$]$_2$ (**5**[$PF_6$]$_2$) complex as an analytically pure sample. Small dark crystals of **5**[$PF_6$]$_2$ could be grown after layering a dichloromethane solution of the complex with *n*-pentane. Yield 94%. FT-IR (KBr, $\nu$ in cm$^{-1}$) 1988 (s, C≡C); 1593 (vs, Ar($A_1$)). Raman ($\nu$, cm$^{-1}$) 2016 (w, C≡C); 1593 (vs, Ar($A_1$)). $^1$H NMR (200 MHz, $CDCl_3$, $\delta$ in ppm) 22.0 ($H_{bip}$); 7.9−6.4 ($H_{dppe}$); 3.8 ($H_{dppe}$); 2.0 ($H_{dppe}$); −2.4 ($H_{dppe}$); −9.7 ($C_5Me_5$); −37.0 ($H_{bip}$).

**Synthesis of the Mononuclear Fe(II) Vinylidene Complex [($\eta^2$-dppe)($\eta^5$-$C_5Me_5$)Fe(=C=CH-4-{($C_6H_4$)-1,1′-($C_6H_5$)})][$PF_6$] (6v-[$PF_6$]).** In a Schlenk tube, 0.22 g of 4-ethynyl-1,1′-biphenyl (1.23 mmol), 0.70 g of ($\eta^2$-dppe)($\eta^5$-$C_5Me_5$)FeCl (1.12 mmol) and 0.22 g of of $KPF_6$ (1.19 mmol) were introduced in 40 mL of a mixture of MeOH/THF (3:1). The dark green suspension was stirred for 16 h. The solvent was removed in vacuo and the residue was extracted with $CH_2C1_2$. The extract was concentrated in vacuo and *n*-pentane was added to precipitate the vinylidene complex [{($\eta^2$-dppe)($\eta^5$-$C_5Me_5$)Fe}(=C=CH-4-{($C_6H_4$)-1,1′-($C_6H_5$)}][$PF_6$] (**6v**[$PF_6$]) as a pale brown powder which was subsequently washed with diethyl ether and dried. Yield 80%. MS (FAB$^+$, *m*-NBA) *m*/*z* 767.2651([M+1]$^+$, 100%), *m*/*z* calc for [$C_{50}H_{47}P_2{}^{56}$-Fe]$^+$ = 767.2659. FT-IR (KBr, $\nu$ in cm$^{-1}$) 1618 (m, Fe=C=C). $^{31}$P NMR (81 MHz, $CDCl_3$, $\delta$ in ppm) 88.3 (s, 2 P, dppe), −143.0 (septuplet, $^1J_{PF}$ = 713 Hz, 1 P, $PF_6$). $^1$H NMR (200 MHz, $CDCl_3$, $\delta$ in ppm) 7.65−7.20 (m, 27 H, $H_{Ar}$); 6.44 (d, 2 H, $H_{Ar}$); 5.17 (t, 1 H, $^4J_{PH}$ = 3.8 Hz, C=C*H*); 2.25−2.85 (2m, 4 H, P$CH_2$); 1.64 (s, 30 H, $C_5Me_5$).

**Synthesis of Mononuclear Fe(II) Alkynyl Complex ($\eta^2$-dppe)-($\eta^5$-$C_5Me_5$)Fe(C≡C-4-{($C_6H_4$)-1,1′-($C_6H_5$)}) (6).** In a Schlenk tube, 0.161 g (0.21 mmol) of vinylidene complex **6v**[$PF_6$], 0.030 g of $^t$BuOK (0.27 mmol) was introduced in ca. 20 mL THF. The dark red solution was stirred for 5 h. The solvent was then removed in vacuo and the residue was extracted with toluene. The extract was concentrated and *n*-pentane was added to precipitate the ($\eta^2$-dppe)($\eta^5$-$C_5Me_5$)Fe(C≡C-4-{($C_6H_4$)-1,1′-($C_6H_5$)}) complex (**5**) as an orange powder which was subsequently dried in vacuo. Yield 92%. Red crystals of **5** could be grown after layering a dichloromethane solution of the complex with *n*-pentane. MS (FAB$^+$, *m*-NBA) *m*/*z* 766.2597 ([M]$^+$, 100%), *m*/*z* calc for [$C_{50}H_{46}P_2{}^{56}$Fe]$^+$ = 766.2581. Anal. Calcd. For $C_{50}H_{48}P_2Fe$: C, 78.33; H, 6.31. Found: C, 78.32; H, 6.28. FT-IR (KBr, $\nu$ in cm$^{-1}$) 2056 (vs, C≡C); 1594 (s, Ar($A_1$)). Raman ($\nu$, cm$^{-1}$) 2059 (m, C≡C); 1597 (vs, Ar($A_1$)). $^{31}$P NMR (81 MHz, $C_6D_6$, $\delta$ in ppm) 101.5 (s, 2 P, dppe). $^1$H NMR (200 MHz, $CD_2Cl_2$, $\delta$ in ppm) 7.97 (m, 4 H, $H_{Ar}$); 7.60−7.20 (m, 19 H, $H_{Ar}$); 6.75 (d, 2 H, $H_{Ar}$); 2.75−2.03 (2 m, 4 H, P$CH_2$); 1.46 (s, 15 H, $C_5Me_5$). $^{13}$C NMR (125 MHz, $CDCl_3$, $\delta$ in ppm) 139.3 (t, $^2J_{CP}$ = 39 Hz, Fe-*C*≡C); 138.4−126.6 (16 s, $C_{Ar}$); 121.3 (s, Fe−C≡*C*); 88.2 (s, $C_5Me_5$); 29.5 (m, P$CH_2$); 10.1 (s, $C_5Me_5$).

**Synthesis of the Mononuclear Alkyny1 Fe(III) Complex [($\eta^2$-dppe)($\eta^5$-$C_5Me_5$)Fe(C≡C-4-{($C_6H_4$)-1,1′-($C_6H_5$)}][$PF_6$] (6[$PF_6$]).** To a suspension of 0.25 g of the bis alkynyl complex **6** (0.33 mmol), 0.10 g of [Fe($\eta^5$-$C_5H_5$)$_2$][$PF_6$] (0.30 mmol) was added in 15 mL dichloromethane, resulting in an instantaneous darkening of the solution. Stirring was maintained 3 h at room temperature and the solution was concentrated in vacuo to ca. 5 mL. Addition of 50 mL of *n*-pentane allowed precipitation of a dark solid. Decantation, subsequent washing with 2 × 3 mL portions diethyl ether and drying under vacuum yielded the desired [{($\eta^2$-dppe)($\eta^5$-$C_5Me_5$)Fe}(C≡C-4-{($C_6H_4$)-1,1′-($C_6H_5$)}]-[$PF_6$] complex (**6**[$PF_6$]) as an analytically pure sample. Yield 91%. FT-IR (KBr, $\nu$ in cm$^{-1}$) 1989 (s, C≡C); 1599 (vs, Ar($A_1$)). $^1$H NMR (200 MHz, $CDCl_3$, $\delta$ in ppm) 31.0 ($H_{bip}$); 11.0 ($H_{bip}$); 8.0−6.3 ($H_{dppe}$); 3.7 ($H_{dppe}$); 0.9 ($H_{dppe}$); −0.2 ($H_{bip}$); − 0.6 ($H_{bip}$); −2.8 ($H_{dppe}$); −10.4 ($C_5Me_5$); −44.0($H_{bip}$).

**Synthesis of the Mononuclear Alkyny1 Fe(III) Complex [($\eta^2$-dppe)($\eta^5$-$C_5Me_5$)Fe(C≡C-4-{($C_6H_4$)-1,1′-($C_6H_5$)}][TCNQ] (6[TCNQ]).** To a suspension of 0.210 g of the alkynyl complex **6** (0.27 mmol) in 15 mL of THF, 0.055 g of TCNQ (0.27 mmol) was added, resulting in an instantaneous darkening of the solution. Stirring was maintained 3 h at room temperature and the green solution was concentrated in vacuo to ca. 5 mL. Addition of 50 mL of *n*-pentane allowed precipitation of a dark solid. Decantation and subsequent washing with 2 × 3 mL portions of *n*-pentane and drying under vacuum yielded the desired [{($\eta^2$-dppe)($\eta^5$-$C_5Me_5$)Fe}(C≡C-4-{($C_6H_4$)-1,1′-($C_6H_5$)}][TCNQ] complex (**6**[TCNQ]). Yield 90%. Small dark crystals of **6**[TCNQ] could be grown after layering a dichloromethane solution of the complex with *n*-pentane.

**Electrochemical Experiments.** All the cyclic voltammetry experiments were carried out at 20 ± 0.1 °C using a cell equipped with a jacket allowing circulation of water from the thermostat. The working electrode was either a 1 mm diameter platinum or gold disk. It was carefully polished before each set of voltammograms with 1 $\mu$m diamond paste and ultrasonically rinsed in absolute ethanol. Electrochemical instrumentation consisted of a Tacussel GSTP4 programmer and of home-built potentiostat equipped with a positive feedback compensation device.[61] The data were acquired with a 310 Nicolet oscilloscope. The counter electrode was a Pt wire and the reference electrode an aqueous saturated calomel electrode with a salt bridge containing the supporting electrolyte. The SCE electrode was checked against the ferrocene/ferricinium couple (considering the following $E°$ values: $E°$ = +0.460V/SCE in dichloromethane) before and after each experiment.

Numerical simulations of the voltammograms were performed with the commercial BAS Digisim Simulator 3.1[62] using the default numerical options with the assumption of planar diffusion. At low scan rate, the convection effect was taken into account by considering a pseudo hydrodynamic-diffusion regime (w = 1.4 rad s$^{-1}$, vk = 0.001 cm$^2$s$^{-1}$). Butler−Volmer law was considered for the electron-transfer kinetics transfer. The transfer coefficient, $\alpha$, was taken as 0.5 with equal diffusion coefficients for the all the species ($D$ = 10$^{-5}$ cm$^2$.s$^{-1}$).

**Crystallography.** Crystals of **5**·($C_4H_8O$)·3/4($C_5H_{12}$), **5**[$PF_6$]$_2$·2($CH_2$-$Cl_2$), **6** and **6**[TCNQ]·1/4($CH_2Cl_2$) were obtained as described above. The samples were studied on a NONIUS Kappa CCD with graphite monochromatized MoK$\alpha$ radiation. The cell parameters were obtained with Denzo and Scalepack with 10 frames (psi rotation: 1° per

(61) Garreau, D.; Savéant, J.-M. *J. Electroanal. Chem.* **1972**, *35*, 309−331.
(62) Rudolph, M.; Reddy, D. P.; Felberg, S. W. *Anal. Chem.* **1994**, *66*, 589A-560A.

frames).[63] The data collection[64] ($2\theta_{max}$, number of frames, Ω rotation, scan rate and HKL range are given in Table 7) provided reflections for **5**·($C_4H_8O$)·3/4($C_5H_{12}$), **5**[$PF_6$]$_2$·2($CH_2Cl_2$), **6** and **6**[TCNQ]·1/4($CH_2Cl_2$). Subequent data reduction with Denzo and Scalepack[63] gave the independent reflections (Table 7). The structures were solved with SIR-97 which revealed the non-hydrogen atoms.[65] After anisotropic refinement, the remaining atoms were found in Fourrier difference maps. The complete structures were then refined with SHELXL97[66] by the full-matrix least-squares technique (use of *F* square magnitude; *x*, *y*, *z*, $\beta_{ij}$ for Fe, P, C, N, and/or O atoms, *x*, *y*, *z* in riding mode for H atoms with variables "*N*(var.)", observations and "w" used as defined in Table 7). Atomic scattering factors were taken from the literature.[67] ORTEP views of **5**, $\mathbf{5}^{2+}$, **6** and **6**[TCNQ] were realized with PLATON98.[68]

**Acknowledgment.** We thank J.-Y. Thépot for experimental assistance in the ESR measurements and the CNRS for financial support.

**Supporting Information Available:** Figure showing the superposition of the simulated and experimental CVs of **5**. Tables of selected bond lengths and angles for **5**, **5**[$PF_6$]$_2$, **6** and **6**[TCNQ]. Figures of one alternative (vibronic progression) deconvolution and of the solvent-induced changes of the NIR absorption of **3**[$PF_6$]. A plot of log($H_{ab}$) vs number of bonds between iron atoms. Full details of the X-ray structures of **5** crystallized from nitrobenzene-diethyl ether mixtures, including tables of atomic positional parameters, bond distances and angles, anisotropic and isotropic thermal displacement parameters (25 pages, print/PDF). The CIF files **5**·($C_4H_8O$)·3/4($C_5H_{12}$), **5**[$PF_6$]$_2$·2($CH_2Cl_2$), **6** and **6**[TCNQ]·1/4($CH_2Cl_2$). This material is available free of charge via the Internet at http://pubs.acs.org.

JA057665R

(63) Otwinowski, Z.; Minor, W. In *Methods in Enzymology*; Carter, C. W., Sweet, R. M., Eds.; Academic press: London, 1997; Vol. 276, pp 307−326.
(64) Nonius, B. V. *Kappa CCD Software*; Delft: The Netherlands, 1999.
(65) Altomare, A.; Burla, M. C.; Camalli, M.; Cascarano, G.; Giacovazzo, C.; Guagliardi, A.; Moliterni, A. G. G.; Polidori, G.; Spagna, R. *J. Appl. Chem.* **1998**, *31*, 74−77.
(66) Sheldrick, G. M. *SHELX97−2. Program for the refinement of crystal structures*; University of Göttingen: Germany, 1997.
(67) Reidel: D. *International Tables for X-ray Crystallography*; Kynoch Press: present distrib. D. Reidel, Dordrecht: Birmingham, 1974; Vol. IV.
(68) Spek, A. L. *PLATON. A Multipurpose Crystallographic Tool*; Utrecht University: Utrecht, The Netherlands, 1998.